

1 **Stable isotopes confirm the Banwell Bone Cave Mammal Assemblage Zone**
2 **represents a MIS 5 fauna.**

3
4 Rhiannon E. Stevens* and Hazel Reade

5 Institute of Archaeology, University College London, 31-34 Gordon Square, London,
6 WC1H 0PY, UK.

7
8 *Corresponding author's e-mail: Rhiannon.stevens@ucl.ac.uk

9
10 **Abstract:**

11 The position of the Banwell Bone Cave mammal assemblage zone (MAZ) in the
12 mammalian biostratigraphy of the British Isles has been the focus of debate for
13 decades. Dominated by fauna typical of cold environments it was originally linked to
14 the marine isotope stage (MIS) 4 stadial (c. 72-59 ka). Subsequently it was argued
15 that the Banwell Bone Cave MAZ more likely relates to the temperate interstadial of
16 marine isotope stage (MIS) 5a (c. 86–72 ka). It is envisioned that 'cold fauna' such as
17 bison and reindeer moved into Britain during stadial MIS 5b (c. 90 ka) and were
18 subsequently isolated by the rising sea level during MIS 5a. Here we investigate
19 environmental conditions during the Banwell Bone Cave MAZ using bone collagen
20 $\delta^{13}\text{C}$ and $\delta^{15}\text{N}$ and tooth enamel $\delta^{18}\text{O}$ and $\delta^{13}\text{C}$ isotope analysis. We analyse bison
21 and reindeer from the MAZ type site, Banwell Bone Cave. Our results show
22 unusually high $\delta^{15}\text{N}$ values, which we ascribe to arid conditions within a temperate
23 environment. Palaeo-temperature estimates derived from enamel $\delta^{18}\text{O}$ indicate warm
24 temperatures, similar to present day. These results confirm that the Banwell Bone
25 Cave MAZ relates to a temperate interstadial and supports its correlation to MIS 5a
26 rather than MIS 4.

27
28 **Keywords:** MIS 5a, stable isotope, carbon, nitrogen, oxygen, collagen, enamel,
29 reindeer, bison, British Isles, Stage 5.

30
31 **Introduction:**

32 Mammalian biostratigraphy focuses on correlating and sequencing geological
33 deposits based on the fossil mammal assemblages contained within them. Mammals
34 are good biostratigraphic indicators due to their rapid morphological evolution and
35 turnover (Schreve, 1997). Quaternary climate fluctuation has resulted in major shifts
36 in the biogeography of many mammal species, resulting in discernible patterns of

37 presence and absence in the fossil record of certain regions (Schreve, 1997).
38 Curren and Jacobi (1997, 2001, 2002) outlined a mammalian biostratigraphic
39 framework for the Late Pleistocene in the British Isles that described five mammal
40 assemblage-zones (MAZ; distinctive fossil mammal bone assemblages), including
41 the Banwell Bone Cave MAZ (hereafter the BBC MAZ). Named after the type-site,
42 Banwell Bone Cave in Banwell, Somerset (Figure 1), the BBC MAZ is characterized
43 by a low diversity fauna which consists primarily of tundra species. Reindeer
44 (*Rangifer tarandus*) and bison (*Bison priscus*) dominate the fauna, with mountain
45 hare (*Lepus timidus*), wolf (*Canis Lupus*), wolverine (*Gulo gulo*), and brown bear
46 (*Ursus arctos*) being consistently present (Curren and Jacobi, 2001). Horse (*Equus*
47 *ferus*) and traces of human presence are notably absent from this MAZ. The small
48 mammal fauna from the BBC MAZ is restricted to a single species, the northern vole
49 (*Microtus oeconomus*) (Curren and Jacobi 2011), which today inhabits a broad
50 range of habitats including tundra, mixed forest, taiga and forest steppe biomes.
51
52 The BBC MAZ is known from locations widespread throughout England and Wales
53 (Figure 1). Curren and Jacobi (2001:1710) argued that the BBC MAZ is 'clearly the
54 vertebrate assemblage of a cold environment' and postulated that it correlated
55 closely with the early part of the last cold stage, marine isotope stage 4 (MIS 4).
56 However, in subsequent publications Gilmour *et al.* (2007) and Curren and Jacobi
57 (2011) questioned this correlation and suggested that the BBC MAZ might actually
58 relate to interstadial MIS 5a (the Brimpton interstadial dating to approximately 86–72
59 ka, Worsley *et al.* 1983, Bryant *et al.* 1983). Although typically characteristic of a
60 fauna indicating cold tundra environments, many of the sites that contain the BBC
61 MAZ also contain associated environmental proxies that indicate temperate climates,
62 more characteristic of interstadial conditions. At Willment's Pit, Isleworth, Greater
63 London, fossil Coleoptera provide evidence of interstadial climatic conditions (Coope
64 and Angus, 1975), while pollen and plant macrofossils indicate vegetation
65 dominated by herbaceous species typical of grasslands that occur in treeless
66 landscapes (Kerney *et al.* 1982). At Cassington in Oxfordshire, Coleoptera and
67 pollen provide evidence of an interstadial open tundra environment, with vegetation
68 dominated by Arctic steppe/tundra herbaceous species (Maddy *et al.* 1998). Amino
69 acid racemization dating has tentatively correlated these deposits with MIS 5c and
70 MIS 5a, respectively (Penkman *et al.* 2011, 2013). Further, TIMS dating of stalagmite
71 flowstone enclosing the BBC MAZ at Stump Cross Caverns in North Yorkshire, gave
72 a date of 73.86 +1.20/-1.19 kyr, supporting an interstadial MIS 5a correlation for this
73 assemblage (Gilmour *et al.* 2007).

74

75 Evidence from raised beaches, which indicate higher sea levels, suggest Britain was
76 not joined to continental Europe for most of MIS 5 (Keen 1995). Gilmour *et al.* (2007)
77 and Carrant and Jacobi (2011) argue that the temperate faunal species typical of
78 interglacial conditions survived in Island Britain up until MIS 5c, then during cold MIS
79 5b Britain became temporarily reconnected to the continent and a major faunal
80 change occurred, with the loss of most temperate mammal species and the gain of
81 species typical of arctic conditions (arctic fox (*Vulpes lagopus*), wolverine (*Gulo*
82 *gulo*), and reindeer (*Rangifer tarandus*)). With the onset of MIS 5a, they argue that
83 the new fauna became trapped in Britain by the higher sea-levels and the return of
84 Britain to being an island. The presence of a faunal assemblage typical of cold
85 conditions, alongside palaeoclimate indicators of interstadial conditions, a restricted
86 range of species and the absence of woolly mammoth (*Mammuthus primigenius*),
87 wild horse (*Equus ferus*), woolly rhinoceros (*Coelodonta antiquitatis*), hominin
88 remains and archaeology, which are present in MIS 5a on the European continent
89 are all suggested to be evidence of Britain being an island isolated from the continent
90 at this time (Carrant and Jacobi 2011).

91

92 The possibility that the BBC MAZ represent fauna typical of cold environments living
93 in temperate conditions has implications both for the technique of mammalian
94 biostratigraphy and for our understanding of the Quaternary history of the British
95 Isles. Thus, further investigation is required to confirm whether the BBC MAZ relates
96 to cold or temperate environmental conditions. Here we undertake stable isotope
97 analysis of bison and reindeer bone and teeth from Banwell Bone Cave in order to
98 establish the environmental context in which these animals lived.

99

100 1.1 Background to stable isotopes:

101 Palaeoclimatic and palaeoenvironmental data can be obtained from fossil tooth
102 enamel and bone through stable isotope analyses. The measured isotopic signals
103 are underpinned by dietary specialisation, animal behaviour and environmental
104 conditions. This approach has enabled the reconstruction of Late Pleistocene
105 palaeoenvironmental conditions at a range of archaeological and palaeontological
106 sites (e.g. Sponheimer and Lee Thorpe, 2003; Hedges *et al.* 2005, Stevens and
107 Hedges, 2004; Drucker *et al.* 2008, 2011; Stevens *et al.* 2008, 2014; Szpak *et al.*
108 2010; Reade *et al.* 2016, 2020a; Fabre *et al.* 2011; Jones *et al.* 2018, 2019; Britton *et*
109 *al.* 2019).

110

111 Skeletal carbon is acquired through the animal's diet and in herbivores is ingested
112 directly from plant tissue (Gannes *et al.* 1997). Within the context of Late Pleistocene
113 Europe, where plants used the C₃ photosynthetic pathway and C₄ and CAM plants
114 were most likely absent (Wißing *et al.* 2016), plant δ¹³C would have been influenced
115 by a variety of climatic/environmental variables such as temperature, precipitation,
116 relative humidity, atmospheric carbon dioxide concentrations and the canopy effect
117 (Heaton, 1999; Kohn, 2010). Thus, faunal δ¹³C reflects underlying environmental
118 conditions, mediated by species-specific dietary behaviours, such as grazing versus
119 browsing (Heaton, 1999). Bone collagen δ¹³C signatures primarily reflect dietary
120 protein whereas enamel carbonate δ¹³C reflects the whole diet (Ambrose and Norr,
121 1993). Relative to the plants consumed, herbivore bone collagen δ¹³C (δ¹³C_{coll}) are
122 approximately +5‰ enriched and enamel carbonate δ¹³C (δ¹³C_{enamel}) are
123 approximately +14‰ enriched (Lee Thorpe *et al.* 1989; Cerling and Harris, 1999).
124 Nutritional stress has also been suggested to influence animal δ¹³C values but the
125 evidence for this is equivocal (Doi *et al.* 2017).

126

127 Herbivore nitrogen is acquired from the plants in the animal's diet (Gannes *et al.*
128 1997). Globally, plant δ¹⁵N has been shown to increase with decreasing mean annual
129 precipitation, with plants growing in arid locations having higher δ¹⁵N values than
130 those growing in wetter locations (Austin and Vitousek, 1998; Handley *et al.* 1999;
131 Amundson *et al.* 2003; Szpak, 2014). Furthermore, plant δ¹⁵N values have been
132 shown to be positively correlated with local temperatures, with plants growing in
133 cooler ecosystems have lower δ¹⁵N values than those growing in warmer
134 ecosystems (Martinelli *et al.* 1999; Amundson *et al.* 2003; Pardo *et al.* 2006; Szpak
135 2014). However, at mean annual temperatures of <-0.5°C the relationship between
136 temperature and plant δ¹⁵N deteriorates (Craine *et al.* 2009). The relationships
137 between plant δ¹⁵N and climatic variables are thought to be linked to mycorrhizal
138 associations, N availability and greater relative importance of fractionating losses of
139 N in hot, dry ecosystems compared to cold, wet ecosystems (Craine *et al.* 2015). As
140 for carbon, the δ¹⁵N signatures of the vegetation are passed on to the herbivore
141 consumers and are recorded in their body tissues. Thus herbivore δ¹⁵N reflect the
142 underlying environmental conditions. Relative to the plants consumed, herbivore
143 bone δ¹⁵N are typically +3 to 5‰ enriched (Bocherens and Drucker, 2003).
144 Nutritional stress can also affect animal δ¹⁵N, but the direction and magnitude of
145 these effects depends on whether the animal is undergoing protein catabolism when
146 they are starving or relying more heavily on fat reserves or other processes that

147 conserve protein during fasting (Hobson *et al.* 1993; Polischuk *et al.* 2001; Cherel *et al.*
148 *et al.* 2005; Fuller *et al.* 2005; Mekota *et al.* 2006; Lohuis *et al.* 2007; Newsome *et al.*
149 2010; Bowes *et al.* 2014; Gomez-Campos *et al.* 2011; Aguilar *et al.* 2014, Fleming *et al.*
150 *et al.* 2018).

151

152 Oxygen isotopes in mammal tooth enamel is linked to prevailing climatic and
153 environmental conditions in the vicinity of the animal's habitat during the period of
154 tooth formation (see Pederzani and Britton, 2019 for review). For most species,
155 drinking water is typically the largest source of O to the $\delta^{18}\text{O}$ signature, but water
156 contained in the diet and respiration also contribute (Bryant *et al.* 1995; Luz *et al.*
157 1984; Longinelli 1984; Luz and Kolodny, 1985). The relative contribution that each of
158 these pools makes to an animal's body water depends on the physiological and
159 behavioural characteristics of the species (Kohn, 1996; Kohn *et al.* 1996; Podlesak *et al.*
160 *et al.* 2008; Pederzani and Britton, 2019). For bison and reindeer (obligate drinkers and
161 the species of focus in this study) empirical relationships between skeletal $\delta^{18}\text{O}$ and
162 the $\delta^{18}\text{O}_{\text{precip}}$ have been demonstrated (Hoppe, 2006; Longinelli *et al.* 2003), which in
163 turn displays a strong relationship to surface air temperatures in mid and high latitude
164 environments (Rozanski, 1993). Here we measure $\delta^{18}\text{O}$ in tooth enamel carbonate.
165 In medium-large sized mammals tooth formation typically lasts several months to a
166 few years, thus a sample of enamel can provide information at either an annual or
167 sub-annual resolution (Fricke *et al.* 1996).

168

169 **Methods:**

170 Ten bison and eleven reindeer bones along with eight bison and ten reindeer teeth
171 were sampled for isotope analysis. All specimens came from the 2007 excavations at
172 Banwell Bone Cave led by Roger Jacobi and Andy Carrant as part of the Ancient
173 Human Occupation of Britain (AHOB) project (Ashton and Stringer 2011). As the
174 excavation was limited in size the recovered faunal assemblage was relatively small
175 and it was not possible to select a single skeletal element to ensure any individual
176 was only sampled once. However, the assemblage is thought to be a result of post-
177 depositional mass movement as the bones were completely mixed, directly
178 articulating elements were absent, and parts of the same animal did not occur even
179 vaguely together within the sediments (Carrant and Jacobi, 2011). Details of skeletal
180 elements sampled are given in supplementary files 1 and 2. The reindeer teeth
181 sampled include six teeth found *in situ* in their mandibular bones (three left
182 mandibles, two teeth per mandible), thus a minimum of 3 individuals is represented.

183

184 *2.1 Collagen extraction and analysis*

185 Collagen was extracted from the bison and reindeer bone samples using a modified
186 Longin (1971) method. Chunks of bone were cut using a dental drill with a small
187 cutting wheel attachment. Each sample was cleaned by abrasion with aluminium
188 oxide prior to collagen extraction. Bones were demineralised in 0.5M hydrochloric
189 acid at 4°C until they had completely decalcified. Samples were then rinsed three
190 times with deionized water and gelatinised in a pH3 aqueous solution for 48 hours at
191 75°C. The filtered supernatant containing the soluble collagen was then collected,
192 frozen, and lyophilized. The collagen was weighed into tin capsules for $\delta^{13}\text{C}$ and $\delta^{15}\text{N}$
193 analysis. Analysis was performed at the Godwin Laboratory, Department of Earth
194 Sciences, University of Cambridge, using a Costech automated elemental analyser
195 coupled to a Finnigan MAT253 isotope ratio mass spectrometer. Samples were
196 analysed in duplicate, with carbon and nitrogen results being reported using the delta
197 scale in units of 'per mil' (‰) relative to internationally accepted standards, VPDB
198 and AIR respectively (Hoefs, 2009). Based on replicate analyses of international and
199 laboratory standards, precision is better than $\pm 0.2\text{‰}$ for both $\delta^{13}\text{C}$ and $\delta^{15}\text{N}$.

200

201 *2.2 Enamel carbonate preparation and analysis*

202 The tooth surfaces were cleaned with a brush and then lightly abraded using a
203 tungsten drill bit. The enamel surface of each tooth was abraded from the apex to the
204 cervix of the crown with a diamond-incrusted drill bit and the removed powder
205 sample collected for analysis. Enamel powder samples were prepared according to
206 Balasse *et al.* (2002). Samples were treated with 2–3% NaOCl for 24 hours
207 (0.1ml/mg sample) then repeatedly rinsed with distilled water. Next 0.1 M acetic acid
208 (0.1ml/mg sample) was added to the enamel powder and left for 4 hours. Samples
209 were then thoroughly rinsed, frozen, and lyophilized. $\delta^{18}\text{O}$ and $\delta^{13}\text{C}$ analysis was
210 performed at the Godwin Laboratory, Department of Earth Sciences, University of
211 Cambridge. Samples were reacted with 100% orthophosphoric acid for 10 minutes at
212 90°C in individual vessels in an automated cryogenic distillation system (PRISM),
213 interfaced with a Finnigan MAT 253 isotope ratio mass spectrometer. Results are
214 reported with reference to the international standard VPDB calibrated through the
215 NBS19 standard (Coplen 1995) and the precision is better than $\pm 0.10\text{‰}$ for both $\delta^{18}\text{O}$
216 and $\delta^{13}\text{C}$.

217

218 **Results:**

219 *Collagen carbon and nitrogen:*

220 Collagen was successfully extracted from all bones and had C/N atomic ratios
221 between 2.9 and 3.6, which indicates good collagen preservation (DeNiro, 1985).
222 The $\delta^{13}\text{C}_{\text{coll}}$ and $\delta^{15}\text{N}$ values of bison and reindeer are listed in supplementary file 1
223 and shown in figure 2. Additional published bison $\delta^{13}\text{C}_{\text{coll}}$ and $\delta^{15}\text{N}$ data from two
224 specimens from Banwell Bone Cave were added to the dataset (Higham *et al.* 2006).
225 Bison $\delta^{13}\text{C}_{\text{coll}}$ values range from -21.4‰ to -20.3‰ with a mean of -20.7 ± 0.3 ‰ and
226 $\delta^{15}\text{N}$ values range from 9.1‰ to 10.8‰ with a mean of 9.8 ± 0.5 ‰. Reindeer $\delta^{13}\text{C}_{\text{coll}}$
227 values are higher than those of the bison, ranging from -19.9‰ to -19.6‰ with a
228 mean of -19.8 ± 0.1 ‰, whereas reindeer $\delta^{15}\text{N}$ values are generally lower and more
229 variable than those of the bison, ranging from 5.8‰ to 9.2‰ with a mean of 7.4 ± 1.3
230 ‰. Mann-Whitney U tests show there is a significant difference between bison and
231 reindeer $\delta^{15}\text{N}$ ($W=128, p < 0.001$) and $\delta^{13}\text{C}_{\text{coll}}$ ($W=0, p < 0.001$).

232

233 *Tooth carbonate carbon and oxygen:*

234 Tooth $\delta^{13}\text{C}_{\text{enamel}}$ and $\delta^{18}\text{O}_{\text{enamel}}$ results are listed in supplementary file 2. Mean bison
235 $\delta^{13}\text{C}_{\text{enamel}}$ is -11.5 ± 1.0 ‰, with individual values ranging from -10.1 to -12.6 ‰. As
236 with the $\delta^{13}\text{C}_{\text{coll}}$ results, reindeer mean $\delta^{13}\text{C}_{\text{enamel}}$ is greater than that of the bison,
237 being -10.5 ± 0.4 ‰. However, unlike the collagen, there is some overlap in reindeer
238 and bison $\delta^{13}\text{C}_{\text{enamel}}$ values (Figure 3). Less variability is seen in reindeer
239 $\delta^{13}\text{C}_{\text{enamel}}$ (ranging from -10.1 to -11.0 ‰) than in that of the bison. $\delta^{18}\text{O}$ values range
240 from -7.0 to -5.7 ‰ for bison (mean = -6.5 ± 0.4 ‰) and -8.2 to -5.0 ‰ for reindeer
241 (mean = -6.6 ± 1.3 ‰). Mann-Whitney U tests show there is no significant difference
242 between bison and reindeer $\delta^{13}\text{C}_{\text{enamel}}$ ($W=25, p > 0.05$) or $\delta^{18}\text{O}$ ($W=40, p > 0.05$).

243

244 *Data conversions:*

245 To facilitate direct comparison, $\delta^{13}\text{C}_{\text{coll}}$ and $\delta^{13}\text{C}_{\text{enamel}}$ were converted to $\delta^{13}\text{C}_{\text{diet}}$ by
246 assuming a diet to collagen offset of +5‰, and diet to carbonate offset of +14‰
247 following Lee Thorpe *et al.* 1989 and Cerling and Harris 1999 (Figure 4,
248 supplementary file 3). No significant difference was seen between estimated $\delta^{13}\text{C}_{\text{diet}}$
249 values reconstructed from tooth enamel and bone collagen for either bison (Mann-
250 Whitney U test, $W=44, p > 0.05$) or reindeer (Mann-Whitney U test, $W=46, p > 0.05$).

251

252 To facilitate palaeo-drinking water estimates, we first converted $\delta^{18}\text{O}_{\text{enamel}}$ results from
253 the V-PDB to the V-SMOW scale following (Coplen, 2011):

$$254 \quad \delta^{18}\text{O}_{\text{VSMOW}} = 1.03091 * \delta^{18}\text{O}_{\text{VPDB}} + 30.91$$

255

[1]

256 To estimate drinking water $\delta^{18}\text{O}$ for bison, we invert the empirically derived
257 relationship between tooth enamel carbonate $\delta^{18}\text{O}$ ($\delta^{18}\text{O}_{\text{carb}}$) and local environmental
258 water ($\delta^{18}\text{O}_{\text{envi}}$) given in Hoppe (2006) using the method recommended by Pryor *et*
259 *al.* (2014):

260

$$\delta^{18}\text{O}_{\text{envi}} = (\delta^{18}\text{O}_{\text{carb}} - 30.057 (\pm 0.58)) / 0.703 (\pm 0.12) \quad [2]$$

263 For reindeer, we use a modified version of the relationship between skeletal
264 phosphate $\delta^{18}\text{O}$ ($\delta^{18}\text{O}_{\text{phos}}$) and local environmental water ($\delta^{18}\text{O}_{\text{envi}}$) presented in
265 Longinelli *et al.* (2003). Longinelli *et al.*'s dataset includes both tooth and bone
266 samples and we note the relationship between $\delta^{18}\text{O}_{\text{phos}}$ and $\delta^{18}\text{O}_{\text{envi}}$ differs between
267 the two sample types. In our study we have analysed only tooth enamel, so we
268 derive a relationship between $\delta^{18}\text{O}_{\text{phos}}$ and $\delta^{18}\text{O}_{\text{envi}}$ based only on the tooth enamel
269 data reported in Longinelli *et al.* (2003). Using inverted least-square regression
270 (Pryor *et al.* 2014) the relationship between $\delta^{18}\text{O}_{\text{envi}}$ and $\delta^{18}\text{O}_{\text{phos}}$ is given by:

271

$$\delta^{18}\text{O}_{\text{envi}} = (\delta^{18}\text{O}_{\text{phos}} - 20.117 (\pm 0.34)) / 0.683 (\pm 0.11) \quad [3]$$

274 As this equation was derived for $\delta^{18}\text{O}_{\text{phos}}$, and we analysed the carbonate phase of
275 enamel a conversion between the two bioapatite structures is required. $\delta^{18}\text{O}_{\text{carb}}$
276 covaries strongly with $\delta^{18}\text{O}_{\text{phos}}$ and we estimate $\delta^{18}\text{O}_{\text{phos}}$ for our results following
277 Zazzo *et al.* (2004, equation 2):

$$\delta^{18}\text{O}_{\text{phos}} = (0.973 * \delta^{18}\text{O}_{\text{carb}} (\pm 0.01)) - 8.121 (\pm 0.36) \quad [4]$$

279

280
281 The calculated palaeo- $\delta^{18}\text{O}_{\text{envi}}$ values are assumed to provide a satisfactory
282 approximation of local palaeo-precipitation $\delta^{18}\text{O}$ ($\delta^{18}\text{O}_{\text{precip}}$). Assuming the empirical
283 relationship that exists in the modern environment between $\delta^{18}\text{O}_{\text{precip}}$ and mean
284 annual air temperature (e.g. Rozanski *et al.*, 1993) is applicable to the past, palaeo-
285 $\delta^{18}\text{O}_{\text{precip}}$ can be used to estimate palaeo-air temperature. However, this observed
286 relationship is geographically variable. Here, we use the relationship derived from
287 European data originating at sites below 500m of altitude by Pryor *et al.* (2014):

288

$$\text{Temperature (}^\circ\text{C)} = (\delta^{18}\text{O}_{\text{precip}} - 13.74 (\pm 0.16)) / 0.53 (\pm 0.08) \quad [5]$$

289

290

291 Each data conversion has an associated uncertainty. We use the error propagation
292 tool presented in Pryor *et al.* (2014) to calculate the compound uncertainty
293 associated with our palaeo- $\delta^{18}\text{O}_{\text{precip}}$ and palaeotemperature estimates.

294

295 **Discussion**

296 *Carbon:*

297 The bone collagen and tooth enamel $\delta^{13}\text{C}$ values confirm a C_3 plant-based diet,
298 typical of the steppe-tundra grasslands of the Late Pleistocene. The significantly
299 higher reindeer $\delta^{13}\text{C}_{\text{coll}}$ relative to bison $\delta^{13}\text{C}_{\text{coll}}$ (Figure 2) follows a pattern often
300 observed in Late Pleistocene contexts, where reindeer have higher $\delta^{13}\text{C}_{\text{coll}}$ than other
301 contemporary herbivores including bovids, equids and other cervids such as red deer
302 (e.g. Fizet *et al.* 1995; Drucker *et al.* 2003; Stevens *et al.* 2009). This has been
303 attributed to their consumption of lichens, which exhibit higher $\delta^{13}\text{C}$ values than
304 sympatric C_3 vascular plants (Park and Epstein, 1960; Maguas and Brugnoli, 1996;
305 Drucker *et al.* 2001). The overlap of bison and reindeer $\delta^{13}\text{C}_{\text{enamel}}$ values potentially
306 indicates ecological niche overlap and suggests a lichen component in the bovid diet
307 which is not obvious from the $\delta^{13}\text{C}_{\text{coll}}$ values. Lichens are a rich source of
308 carbohydrate and poor source of protein. As $\delta^{13}\text{C}_{\text{enamel}}$ reflect whole diet $\delta^{13}\text{C}$
309 (Ambrose and Norr, 1993; Tieszen and Fagre, 1993) low lichen consumption is more
310 likely to be visible in $\delta^{13}\text{C}_{\text{enamel}}$ than in $\delta^{13}\text{C}_{\text{coll}}$, which primarily reflect dietary protein
311 $\delta^{13}\text{C}$ (Krueger & Sullivan, 1984). Overlap between bovid and reindeer dietary niche
312 and potential lichen consumption by bovids has previously been suggested in other
313 Late Pleistocene contexts (Bocherens *et al.* 2015; Julien *et al.* 2012; Reade *et al.*,
314 2020b), and has been observed also in some modern bison populations (Larter and
315 Gates, 1991). Overlapping reindeer and bison $\delta^{13}\text{C}_{\text{enamel}}$ values could also be
316 produced by species-specific differences in tooth growth and enamel mineralisation
317 rates. A full year of tooth growth is represented in the majority of analysed bison
318 teeth, such that the derived dietary signal will represent an average spanning this
319 time period. In comparison, the majority of the analysed reindeer teeth formed
320 between late spring and autumn, and thus represent a dietary signature biased
321 toward the summer months (see supplementary file 2). In modern reindeer
322 populations, lichen is less heavily relied upon in summer compared to in the winter
323 (Holleman *et al.* 1979). Together tooth and bone $\delta^{13}\text{C}$ data suggest the BBC MAZ
324 was deposited at a time when steppe-tundra grasslands likely covered the local
325 landscape.

326

327 *Nitrogen:*

328 Both the reindeer and bison $\delta^{15}\text{N}$ values are high for herbivore species. Notably the
329 reindeer $\delta^{15}\text{N}$ values are higher than all published Late Pleistocene reindeer $\delta^{15}\text{N}$
330 values from the UK (Figure 5, supplementary file 4). Comparatively high reindeer
331 $\delta^{15}\text{N}$ values are relatively rare in Late Pleistocene Europe but are found in reindeer
332 from southwest France during MIS 3 (Figure 5, Bocherens *et al.* 2014). From the 97
333 Late Pleistocene European bison we found in the published literature, only two
334 examples have $\delta^{15}\text{N}$ values comparative to those observed at Banwell Bone Cave
335 (Figure 6, supplementary file 5). One is from southwest France (Les Pradelles /
336 Marillac $\delta^{15}\text{N} = 9.3\text{‰}$, Fizet *et al.* 1995) and another from Crimea, (Emine-Bair-
337 Khosar, $\delta^{15}\text{N} = 9.1\text{‰}$, Gasirowski *et al.* 2014); both date to MIS 3. Thus, the range
338 in bison $\delta^{15}\text{N}$ observed in the Banwell Bone Cave material is extremely rare for Late
339 Pleistocene Europe.

340

341 Two possible explanations exist for such high herbivore $\delta^{15}\text{N}$ values. First, elevated
342 $\delta^{15}\text{N}$ can be produced by nutritional stress. However, for such high bone collagen
343 $\delta^{15}\text{N}$ to be solely indicative of nutritional stress long periods of fasting/starvation for
344 both reindeer and bison would be required. Given the abundance of the bison and
345 reindeer remains at Banwell Bone Cave and at other site containing the BBC MAZ, it
346 seems that the environment was suitable for long-term co-existence of the two
347 species and does not suggest the environment was so nutritionally poor as to result
348 in significant periods of starvation. Furthermore, where comparable reindeer $\delta^{15}\text{N}$
349 values are seen in southwest France during MIS 3 (Bocherens *et al.* 2014), reindeer
350 were also extremely abundant, often being the dominant fauna in zooarchaeological
351 assemblages (Mellars, 2004). Such abundance is unlikely in an environment in which
352 animals are starving.

353

354 The alternative and most parsimonious explanation is that the elevated reindeer and
355 bison $\delta^{15}\text{N}$ values are linked to environmental conditions. Plant to herbivore $\delta^{15}\text{N}$
356 fractionation has been shown to be constant (Männel *et al.* 2007; Kuitens *et al.*
357 2015; Bocherens *et al.* 2014), and relationships between herbivore $\delta^{15}\text{N}$ and
358 temperature and/or aridity have been shown to be driven by the $\delta^{15}\text{N}$ of the plants
359 the animals consume (Murphy and Bowman, 2006; Hartman, 2011). Today, high
360 plant $\delta^{15}\text{N}$ are linked to low precipitation (aridity) and higher temperatures. However,
361 in southwest France, the high MIS 3 reindeer $\delta^{15}\text{N}$ values were found alongside
362 elevated $\delta^{15}\text{N}$ values in contemporary herbivores and carnivores and were
363 interpreted as being indicative of an environment for which no modern analogue is

364 known. The contemporary palaeoclimate proxies indicated relatively low temperatures,
365 thus the elevated $\delta^{15}\text{N}$ values were ascribed to aridity (Fizet *et al.* 1995; Richards *et al.*
366 *et al.* 2008; Bocherens *et al.* 2014). Similarly, the beetle, pollen and plant macrofossil
367 data from BBC MAZ sites, along with the bison and reindeer oxygen isotope data
368 (see below) do not indicate very high temperatures (Coope and Angus, 1975; Coope
369 *et al.* 1997; Maddy *et al.* 1998). Thus, the Banwell Bone Cave reindeer and bison
370 $\delta^{15}\text{N}$ likely also indicate arid conditions. The rarity of comparable bison $\delta^{15}\text{N}$ values
371 from Late Pleistocene Europe support the notion that the BBC MAZ was deposited
372 under non-analogue environmental conditions.

373

374 *Oxygen:*

375 Mean $\delta^{18}\text{O}_{\text{enamel}}$ values are similar for both species ($-6.5 \pm 0.4 \text{‰}$ for bison and $-6.5 \pm$
376 1.3‰ for reindeer). As with the $\delta^{13}\text{C}_{\text{enamel}}$ and $\delta^{15}\text{N}_{\text{coll}}$, reindeer $\delta^{18}\text{O}_{\text{enamel}}$ is more
377 variable than that of bison, ranging from -8.2 to -5.0‰ , compared to -7.0 to -5.7‰ .
378 The higher variability in the reindeer $\delta^{18}\text{O}_{\text{enamel}}$ is likely attributable to the different
379 time periods each tooth represents, with the bison $\delta^{18}\text{O}_{\text{enamel}}$ values relating to
380 approximately a full annual cycle, and the reindeer $\delta^{18}\text{O}_{\text{enamel}}$ signatures being biased
381 toward the summer months (Supplementary file 2).

382

383 Using the discussed data conversions, we estimate a mean palaeo- $\delta^{18}\text{O}_{\text{precip}}$ of $-8.3 \pm$
384 1.3‰ from the bison data and $-7.0 \pm 1.6 \text{‰}$ from the reindeer data. For individual
385 samples, palaeo- $\delta^{18}\text{O}_{\text{precip}}$ estimates range from -9.1‰ to -7.1‰ for bison and -9.3‰
386 to -4.6‰ for reindeer, with associated uncertainties between 2.4‰ and 2.8‰
387 (Supplementary file 2). For comparison, modern mean annual $\delta^{18}\text{O}_{\text{precip}}$ in the UK
388 ranges from approximately -8.5 to -6.5‰ (IAEA GNIP). Estimated palaeo- $\delta^{18}\text{O}_{\text{precip}}$
389 therefore indicates similar climatic conditions to the present day, i.e. temperate
390 conditions, assuming that $\delta^{18}\text{O}_{\text{precip}}$ can be treated as a function of temperature. The
391 palaeo- $\delta^{18}\text{O}_{\text{precip}}$ estimates made from the reindeer data include values higher than
392 might be expected, and if taken at face value could indicate a climate far warmer
393 than present. However, this conjecture should be treated cautiously. As the majority
394 of our reindeer samples are believed to have formed only over the summer months,
395 the occurrence of higher palaeo- $\delta^{18}\text{O}_{\text{precip}}$ estimates are not actually surprising. In
396 fact, an estimated mean $\delta^{18}\text{O}_{\text{precip}}$ of -4.6‰ is not that dissimilar to modern mean
397 monthly maximum values for the UK of approximately -4.5 to -2.0‰ (IAEA, GNIP).
398 Regardless, the $\delta^{18}\text{O}_{\text{enamel}}$ results only show evidence of $\delta^{18}\text{O}_{\text{precip}}$ values associated
399 with temperate environments, and we find no indication of colder conditions.

400

401 Using species mean palaeo- $\delta^{18}\text{O}_{\text{precip}}$ estimates we derive palaeo-temperature
402 estimates of 10.3 ± 2.5 °C from the bison data and 12.8 ± 3.1 °C from the reindeer
403 data. These temperatures are comparable to the recent (1981-2010) 30-year mean
404 annual air temperature for southwest England of 10.5°C
405 (<https://www.metoffice.gov.uk/>). Similarities are also apparent between our
406 palaeotemperature estimates and others from Late Pleistocene interglacial deposits.
407 Coleoptera-based estimates from lithofacies B at Cassington, which contained a
408 bison-reindeer fauna attributed to the BBC MAZ and has been dated to interstadial
409 MIS 5a, range from 17 - 18 °C for the warmest month to -4 – 4 °C for the coldest
410 month (Maddy, 1998; Penkman 2011, 2013). Comparatively, Coleoptera-based
411 temperature estimates from lithofacies D at the site, correlated to stadial MIS 4,
412 range from 7 - 11 °C for the warmest month to -30 – -10 °C for the coldest month
413 (Maddy, 1998). Likewise, molluscs from the organic silts at Willment's Pit, Isleworth,
414 which also contains mammalian fauna assigned to the BBC MAZ and tentatively
415 correlated to interstadial MIS 5c, suggest mean July temperature of no lower than
416 15°C (Kerney, 1982; Penkman 2011, 2013). Based on these independent data, our
417 palaeo-temperature estimates clearly fall within the expected range of a Late
418 Pleistocene interstadial climate, and outside of the range expected of a Late
419 Pleistocene stadial climate.

420

421 **Conclusion:**

422 The results of the stable isotope analyses conducted in this study confirm that the
423 Banwell Bone Cave faunal assemblage relates to a temperate rather than cold
424 environment. Our study is the first to derive palaeoclimate information directly from
425 the fauna itself, providing evidence that the bison-reindeer fauna, typically thought of
426 as a cold climate assemblage, existed under temperate climate conditions at Banwell
427 Bone Cave. Our results support the correlation of the BBC MAZ to interstadial MIS
428 5a rather than to the succeeding stadial of MIS 4.

429

430 The $\delta^{13}\text{C}$ values of bison and reindeer fauna indicate C_3 plant-based diets, typical of
431 the steppe-tundra grasslands of the Late Pleistocene. Lichen appears to have been
432 important for reindeer and potentially also a component of the bison diet, thus
433 indicating some possible ecological niche overlap. The $\delta^{15}\text{N}$ values of both bison and
434 reindeer are unusually high and likely represent arid conditions within a temperate
435 environment. Mean palaeo-temperature estimates derived from bison and reindeer
436 tooth enamel $\delta^{18}\text{O}$ indicate that temperate conditions similar to the present day
437 prevailed during the deposition of the fauna at Banwell Bone Cave.

438

439 Confirmation that fauna from the Banwell Bone Cave lived in conditions consistent
440 with the temperate interstadial MIS 5a rather than the succeeding cool stadial MIS 4,
441 lends support to the hypothesis that the BBC MAZ represents an island fauna and
442 that a mismatch between British and other European mammal faunas existed during
443 MIS 5 (Gilmour *et al.* 2007). Finally, this study provides a cautionary tale for the use
444 of particular species as climatic indicators. The presence or absence of geographical
445 barriers may substantially influence the species composition of a faunal assemblage
446 to the extent that species may have existed in environments beyond their current
447 environmental limits, or in environments for which there are no modern analogues.

448

449 **Acknowledgments:**

450 RS and HR are funded by an ERC consolidator grant to RS (ERC-CG-617777: UP-
451 North). We thank Delfin Weis and Elizabeth Rutherford for assistance with sample
452 preparation and James Rolfe for assistance with analysis. We are grateful to
453 Delphine Fremondeau for assistance with ZooMs analysis. Rebecca Kearney is
454 thanked for assistance with formatting. We are very grateful to Andy Carrant and the
455 late Roger Jacobi for providing newly excavated material for analysis and for
456 encouraging us to undertake research on the Late Pleistocene fauna of the British
457 Isles. The excavations at Banwell Bone Cave were conducted as part of the Ancient
458 Human Occupation of Britain (AHOB) Project funded by the Leverhulme Trust.

459

460 **Bibliography:**

461

462 Aguilar, A., Giménez, J., Gómez–Campos, E., Cardona, L., Borrell, A., 2014. $\delta^{15}\text{N}$
463 value does not reflect fasting in mysticetes. PLoS One 9(3), e92288.

464

465 Ambrose, S. H., Norr, L., 1993. Experimental evidence for the relationship of the
466 carbon isotope ratios of whole diet and dietary protein to those of bone collagen and
467 carbonate. In: Lambert, J., Grupe, G. (Eds.), Prehistoric human bone: Archaeology at
468 the molecular level. Springer, New York, pp. 1-37.

469

470 Amundson R., Austin A. T., Schuur E. A. G., Yoo K., Matzek V., Kendall C.,
471 Uebersax, A., Brenner, D. Baisden, W.T., 2003. Global patterns of the isotopic
472 composition of soil and plant nitrogen. Global Biogeochemical Cycles 17(1), 1031.

473

474 Ashton, N.M., Lewis, S.G.,Stringer, C.B. (eds) The Ancient Human Occupation of
475 Britain. Elsevier, Amsterdam.
476

477 Austin A. T., Vitousek P. M., 1998. Nutrient dynamics on a precipitation gradient in
478 Hawai'i. *Oecologia* 113(4), 519–529.
479

480 Balasse, M., Ambrose, S.H., Smith, A.B., Price, T.D., 2002. The seasonal mobility
481 model for prehistoric herders in the South-Western Cape of South Africa assessed
482 by isotopic analysis of sheep tooth enamel. *Journal of Archaeological Science* 29(9),
483 917–932.
484

485 Bocherens, H., Drucker, D., 2003. Trophic level isotopic enrichment of carbon and
486 nitrogen in bone collagen: case studies from recent and ancient terrestrial
487 ecosystems. *International Journal of Osteoarchaeology* 13(1–2), 46–53.
488

489 Bocherens, H., Drucker, D.G., Germonpré, M., Lázničková-Galetová, M., Naito, Y.I.,
490 Wissing, C., Brůžek, J., Oliva, M., 2015. Reconstruction of the Gravettian food-web
491 at Předmostí I using multi-isotopic tracking (¹³C, ¹⁵N, ³⁴S) of bone collagen.
492 *Quaternary International* 359, 211-228.
493

494 Bocherens, H., Drucker, D.G., Madelaine, S., 2014. Evidence for a ¹⁵N positive
495 excursion in terrestrial foodwebs at the Middle to Upper Palaeolithic transition in
496 south-western France: implications for early modern humans. *Journal of Human*
497 *Evolution* 69, 31-43.
498

499 Bowes, R. E., Lafferty, M. H., Thorp, J. H., 2014. Less means more: nutrient stress
500 leads to higher $\delta^{15}\text{N}$ ratios in fish. *Freshwater Biology* 59, 1926–1931.
501

502 Britton, K., Pederzani, S., Kindler, L., Roebroeks, W., Gaudzinski-Windheuser, S.,
503 Richards, M. P., Tütken, T., 2019. Oxygen isotope analysis of Equus teeth evidences
504 early Eemian and early Weichselian palaeotemperatures at the Middle Palaeolithic
505 site of Neumark-Nord 2, Saxony-Anhalt, Germany. *Quaternary Science Reviews*
506 226, 106029.
507

508 Bryant, I.D., Holyoak, D.T., Moseley, K.A., 1983. Late Pleistocene deposits at
509 Brimpton, Berkshire, England. *Proceedings of the Geologists' Association* 94(4),
510 321–343.

511
512 Bryant, J.D. Froelich, P., 1995. A model of oxygen isotope fractionation in body water
513 of large mammals. *Geochimimica et Cosmochimica Acta* 59(21), 4523-4537.
514
515 Cerling, T. E., Harris, J. M., 1999. Carbon isotope fractionation between diet and
516 bioapatite in ungulate mammals and implications for ecological and paleoecological
517 studies. *Oecologia* 120(3), 347-363.
518
519 Cherel, Y., Hobson, K. A., Baiileul, F., Groscolas, R., 2005. Nutrition, physiology, and
520 stable isotopes: new information from fasting and molting penguins. *Ecology* 86(11),
521 2881–2888.
522
523 Coope, G.R., Angus, R.B., 1975. An ecological study of a temperate interlude in the
524 Middle of the Last Glaciation, Based on Fossil Coleoptera from Isleworth, Middlesex.
525 *Journal of Animal Ecology* 44(2), 365-391.
526
527 Coope, G.R., Gibbard, P.L., Hall, A.R., Preece, R.C., Robinson, J.E., Sutcliffe, A.J.,
528 1997. Climatic and environmental reconstructions based on fossil assemblages from
529 Middle Devensian (Weichselian) deposits of the River Thames at South Kensington,
530 Central London, UK. *Quaternary Science Reviews* 16(10), 1163–1195.
531
532 Coplen, T. B., 2011. Guidelines and recommended terms for expression of stable-
533 isotope-ratio and gas-ratio measurement results. *Rapid Communications in Mass*
534 *Spectrometry* 25(17), 2538–2560.
535
536 Coplen, T.B., 1995. Reporting of stable hydrogen, carbon, and oxygen isotopic
537 abundances — (technical report). *Geothermics* 24(5-6), 707-712.
538
539 Craine, J. M., Elmore, A. J., Aidar, M. P. M., Bustamante, M., Dawson, T. E., Hobbie,
540 E. A., *et al.* 2009. Global patterns of foliar nitrogen isotopes and their relationships
541 with climate, mycorrhizal fungi, foliar nutrient concentrations, and nitrogen
542 availability. *New Phytologist* 183(4), 980–992.
543
544 Craine, J.M., Brookshire, E.N.J., Cramer, M.D., Hasselquist, N.J., Koba, K., Marin-
545 Spiotta, E., Wang, L., 2015. Ecological interpretations of nitrogen isotope ratios of
546 terrestrial plants and soils. *Plant and Soil* 396, 1– 26.
547

548 Curren, A., Jacobi, R., 1997. Vertebrate faunas of the British Late Pleistocene and
549 the chronology of human settlement. *Quaternary Newsletter* 82, 1–8.
550

551 Curren, A., Jacobi, R., 2001. A formal mammalian biostratigraphy for the Late
552 Pleistocene of Britain. *Quaternary Science Reviews* 20, 1707–1716.
553

554 Curren, A., Jacobi, R., 2002. Human presence and absence in Britain during the
555 early part of the Late Pleistocene. In: Tuffreau, A., Roebroeks, W. (Eds), *Le Denier*
556 *Interglaciaire et les occupations du Paléolithique moyen*. Publications du CERP no.
557 8, Université des Sciences et technologies de Lille, Villeneuve-d'Ascq, 105–113.
558

559 Curren, A.P., Jacobi, R.M., 2011. The mammalian faunas of the British late
560 Pleistocene. In: Ashton, N.M., Lewis, S.G., Stringer, C.B. (Eds.), *The Ancient Human*
561 *Occupation of Britain*. Elsevier, Amsterdam, pp. 165-180.
562

563 d'Angela, D., Longinelli, A., 1990. Oxygen isotopes in living mammal's bone
564 phosphate: further results. *Chemical Geology: Isotope Geoscience section* 86, 75–
565 82.
566

567 DeNiro, M.J., 1985. Postmortem preservation and alteration of in vivo bone collagen
568 isotope ratios in relation to palaeodietary reconstruction. *Nature* 317(6040), 806-809.
569

570 Doi, H., Akamatsu, F., González, A.L., 2017. Starvation effects on nitrogen and
571 carbon stable isotopes of animals: An insight from meta-analysis of fasting
572 experiments. *Royal Society Open Science* 4(8), 170633.
573

574 Drucker, D., Bocherens, H., Bridault, A., Billiou, D., 2003. Carbon and nitrogen
575 isotopic composition of red deer (*Cervus elaphus*) collagen as a tool for tracking
576 palaeoenvironmental change during the Late-Glacial and Early Holocene in the
577 northern Jura (France). *Palaeography, Palaeoclimatology, Palaeoecology* 195(3-4),
578 375-388.
579

580 Drucker, D., Bocherens, H., Pike-Tay, A., Mariotti, A., 2001. Isotopic tracking of
581 seasonal dietary change in dentine collagen: preliminary data from modern caribou.
582 *Comptes Rendus de l'Académie des Sciences - Series IIA - Earth and Planetary*
583 *Science* 333(5), 303-309.
584

585 Drucker, D.G., Bridault, A., Cupillard, C., Hujic, A., Bocherens, H., 2011. Evolution of
586 habitat and environment of red deer (*Cervus elaphus*) during the Late-glacial and
587 early Holocene in eastern France (French Jura and the western Alps) using multi-
588 isotope analysis ($\delta^{13}\text{C}$, $\delta^{15}\text{N}$, $\delta^{18}\text{O}$, $\delta^{34}\text{S}$) of archaeological remains. *Quaternary*
589 *International* 245(2), 268-278.

590

591 Drucker, D.G., Bridault, A., Hobson, K.A., Szuma, E., Bocherens, H., 2008. Can
592 carbon-13 in large herbivores reflect the canopy effect in temperate and boreal
593 ecosystems? Evidence from modern and ancient ungulates. *Palaeogeography,*
594 *Palaeoclimatology, Palaeoecology* 266(1-2), 69–82.

595

596 Fabre, M., Lécuyer, C., Brugal, J.P., Amiot, R., Fourel, F., Martineau, F., 2011. Late
597 Pleistocene climatic change in the French Jura (Gigny) recorded in the $\delta^{18}\text{O}$ of
598 phosphate from ungulate tooth enamel. *Quaternary Research* 75(3), 605-613.

599

600 Fizet, M., Mariotti, A., Bocherens, H., 1995. Effect of Diet, Physiology and Climate on
601 Carbon and Nitrogen Stable Isotopes of Collagen in a Late Pleistocene anthropic
602 palaeoecosystem: Marillac, Charente, France. *Journal of Archaeological Science*
603 22(1), 67-79.

604

605 Fleming, A.H., Kellar, N.M., Allen, C.D., Kurle, C.M., 2018. The utility of combining
606 stable isotope and hormone analyses in marine megafauna research. *Frontiers in*
607 *Marine Science* 5, 338.

608

609 Fricke, H.C., D'Neil, J.R., 1996. Inter- and intra-tooth variation in the oxygen isotope
610 composition of mammalian tooth enamel phosphate: implications for
611 palaeoclimatological and palaeobiological research. *Palaeogeography,*
612 *Palaeoclimatology, Palaeoecology* 126, 91-99.

613

614 Fuller, B.T., Fuller, J.L., Sage, N.E., Harris, D.A., O'Connell, T.C., Hedges, R.E.,
615 2005. Nitrogen balance and $\delta^{15}\text{N}$: why you're not what you eat during nutritional
616 stress. *Rapid Communications in Mass Spectrometry* 19(18), 2497–2506.

617

618 Gannes, L.Z., Del Rio, C.M., Koch, P., 1998. Natural abundance variations in stable
619 isotopes and their potential uses in animal physiological ecology. *Comparative*
620 *biochemistry and physiology Part A: Molecular & integrative physiology* 119(3), 725–
621 737.

622
623 Gašiorowski, M., Hercman, H., Ridush, B., Stefaniak, K., 2014. Environment and
624 climate of the Crimean Mountains during the Late Pleistocene inferred from stable
625 isotope analysis of red deer (*Cervus elaphus*) bones from the Emine-Bair-Khosar
626 Cave. *Quaternary International* 326, 243-249.
627
628 Gilmour, M., Curren, A.P., Jacobi, R.M., Stringer, C.B., 2007. Recent TIMS dating
629 results from British Late Pleistocene vertebrate faunal localities: Context and
630 interpretation. *Journal of Quaternary Science* 22(8), 793–800.
631
632 Gomez-Campos, E., Borrell, A., Aguilar, A., 2011. Nitrogen and carbon stable
633 isotopes do not reflect nutritional condition in the striped dolphin. *Rapid*
634 *Communication in Mass Spectrometry* 25(9), 1343–1347.
635
636 Handley, L. L., Austin, A. T., Stewart, G. R., Robinson, D., Scrimgeour, C. M., Raven,
637 J. A., Heaton, T.H.E., Schmidt, S., 1999. The ^{15}N natural abundance ($\delta^{15}\text{N}$) of
638 ecosystem samples reflects measures of water availability. *Australian Journal of*
639 *Plant Physiology* 26(2), 185–199.
640
641 Hartman, G., 2011. Are elevated $\delta^{15}\text{N}$ values in herbivores in hot and arid
642 environments caused by diet or animal physiology? *Functional Ecology* 25, 122-131.
643
644 Heaton, T.H.E., 1999. Spatial, species, and temporal variations in the $^{13}\text{C}/^{12}\text{C}$ ratios
645 of C_3 plants: implications for palaeodiet studies. *Journal of Archaeological Science*
646 26(6), 637-649.
647
648 Hedges, R.E.M., Stevens, R.E., Kock, P.L., 2005. Isotopes in bones. In: Leng, M.J.
649 (Ed), *Isotopes in palaeoenvironmental research*, Vol. 10. Springer, Dordrecht, pp.
650 117-145.
651
652 Higham, T. G., Jacobi, R. M., Bronk Ramsey, C., 2006. AMS radiocarbon dating of
653 ancient bone using ultrafiltration. *Radiocarbon* 48(2), 179–195.
654
655 Hobson, K. A., Alisauskas, R. T., Clark, R. G., 1993. Stable-nitrogen isotope
656 enrichment in avian tissues due to fasting and nutritional stress: implications for
657 isotopic analysis of diet. *Condor* 95(2), 388–394.

658

659 Hoefs, J., 2009. Stable isotope geochemistry. Springer, Berlin.

660

661 Holleman, D. F., Luick, R., White, R. G., 1979. Lichen intake estimates for reindeer
662 and caribou during winter. *Journal of Wildlife Management* 43, 192-201.

663

664 Hoppe, K.A. 2006. Correlation between the oxygen isotope ratio of North American
665 bison teeth and local waters: implication for paleoclimatic reconstructions. *Earth
666 Planetary Science Letters* 244 (1-2), 408-417.

667

668 IAEA/WMO, 2019. Global Network of Isotopes in Precipitation. The GNIP Database.
669 Accessible at: <https://nucleus.iaea.org/wiser>

670

671 Jones, J.R., Richards, M.P., Reade, H., de Quirós, F.B., Marín-Arroyo, A.B.,
672 2019. Multi-Isotope investigations of ungulate bones and teeth from El Castillo and
673 Covalejos caves (Cantabria, Spain): Implications for paleoenvironment
674 reconstructions across the Middle-Upper Palaeolithic transition. *Journal of
675 Archaeological Science: Reports* 23, 1029-1042.

676

677 Jones, J.R., Richards, M.P., Straus, L.G., Reade, H., Altuna, J., Mariezkurrena, K.,
678 Marín-Arroyo, A.B., 2018. Changing environments during the Middle-Upper
679 Palaeolithic transition in the eastern Cantabrian Region (Spain): direct evidence from
680 stable isotope studies on ungulate bones. *Scientific Reports* 8, 14842.

681

682 Julien, M.A., Bocherens, H., Burke, A., Drucker, D.G., Patou-Mathis, M., Krotova, O.,
683 Péan, S., 2012. Were European steppe bison migratory? ^{18}O , ^{13}C and Sr intra-tooth
684 isotopic variations applied to a palaeoethological reconstruction. *Quaternary
685 International* 271, 106-119.

686

687 Keen, D.H., 1995. Raised beaches and sea-levels in the English Channel in the
688 Middle and Late Pleistocene: Problems of interpretation and implications for the
689 isolation of the British Isles. In: Preece, R.C. (Ed.), *Island Britain: A Quaternary
690 Perspective*. Geological Society of London Special Publication 96, 63–74.

691

692 Kerney, M.P., Gibbard, P.L., Hall, A.R. and Robinson, J.E., 1982. Middle devensian
693 river deposits beneath the 'upper floodplain' terrace of the river Thames at Isleworth,
694 west London. *Proceedings of the Geologists' Association* 93(4), 385-393.
695

696 Kohn, M.J., 1996. Predicting animal $\delta^{18}\text{O}$: accounting for diet and physiological
697 adaptation. *Geochimica et Cosmochimica Acta* 60(23), 4811-4829.
698

699 Kohn, M.J., 2010. Carbon isotope compositions of terrestrial C3 plants as indicators
700 of (paleo)ecology and (paleo)climate. *Proceedings of the National Academy of*
701 *Science* 107(46), 19691-19695.
702

703 Kohn, M.J., Schoeninger, M.J., Valley, J.W., 1996. Herbivore tooth oxygen isotope
704 compositions: effects of diet and physiology. *Geochimica et Cosmochimica*
705 *Acta* 60(20), 3889-3896.
706

707 Krueger, H.W., Sullivan, C.H., 1984. Models for carbon isotope fractionation between
708 diet and bone. In: Turnland, J., Johnson, P.E. (Eds.), *Stable Isotopes in Nutrition*.
709 American Chemical Society, Washington DC, pp. 205-222.
710

711 Kuitens, M., van Kolfschoten, T. and van der Plicht, J., 2015. Elevated $\delta^{15}\text{N}$ values
712 in mammoths: a comparison with modern elephants. *Archaeological and*
713 *Anthropological Sciences* 7(3), 289–295.
714

715 Larter, N.C., Gates, C.C., 1991. Diet and habitat selection of wood bison in relation to
716 seasonal-changes in forage quantity and quality. *Canadian Journal of Zoology*
717 69(10), 2677-2685.
718

719 Lee-Thorp, J. A., Sealy, J. C., van der Merwe, N. J., 1989. Stable carbon isotope
720 ratio differences between bone collagen and bone apatite and their relationship to
721 diet. *Journal of Archaeological Science* 16(6), 585-599.
722

723 Lohuis, T. D., Harlow, H. J., Beck, T. D. I., 2007. Hibernating black bears (*Ursus*
724 *americanus*) experience skeletal muscle protein balance during winter
725 anorexia. *Comparative Biochemistry and Physiology Part B: Biochemistry and*
726 *Molecular Biology* 147(1), 20–28.
727

728 Longin, R., 1971. New method of collagen extraction for radiocarbon dating. *Nature*

729 230(5291), 241–242.
730
731 Longinelli, A., 1984. Oxygen isotopes in mammal bone phosphate: a new tool for
732 paleohydrological and paleoclimatological research? *Geochimica et Cosmochimica*
733 *Acta* 48(2), 385-390.
734
735 Longinelli, A., Iacumin, P., Davanzo, S., Nikolaev, V., 2003. Modern reindeer and
736 mice: revised phosphate–water isotope equations. *Earth and Planetary Science*
737 *Letters* 214(3-4), 491-498.
738
739 Luz, B., Kolodny, Y., 1985. Oxygen isotope variations in phosphate of biogenic
740 apatites, IV. Mammal teeth and bones. *Earth and Planetary Science Letters* 75(1),
741 29-36.
742
743 Luz, B., Kolodny, Y., Horowitz, M., 1984. Fractionation of oxygen isotopes between
744 mammalian bone-phosphate and environmental drinking water. *Geochimica et*
745 *Cosmochimica Acta* 48(8),1689-1693.
746
747 Maddy, D., Lewis, S.G., Scaife, R.G., Bowen, D.Q., Coope, G.R., Green, C.P.,
748 Hardaker, T., Keen, D.H., Rees-Jones, J., Parfitt, S., Scott, K., 1998. The Upper
749 Pleistocene deposits at Cassington, near Oxford, England. *Journal of Quaternary*
750 *Science: Published for the Quaternary Research Association* 13(3), 205-231.
751
752 Maguas, C., Brugnoli, E. 1996. Spatial variation in carbon isotope discrimination
753 across the thalli of several lichen species. *Plant, Cell & Environment* 19(4), 437- 446.
754
755 Männel, T.T., Auerswald, K., Schnyder, H., 2007. Altitudinal gradients of grassland
756 carbon and nitrogen isotope composition are recorded in the hair of grazers. *Global*
757 *Ecology and Biogeography* 16(5), 583-592.
758
759 Martinelli, L.A., Piccolo, M.D.C., Townsend, A.R., Vitousek, P.M., Cuevas, E.,
760 McDowell, W., Robertson, G.P., Santos, O.C., Treseder, K., 1999. Nitrogen stable
761 isotopic composition of leaves and soil: tropical versus temperate
762 forests. *Biogeochemistry* 46(1-3), 45-65.
763

764 Mekota, A.M., Grupe, G., Ufer, S. and Cuntz, U., 2006. Serial analysis of stable
765 nitrogen and carbon isotopes in hair: monitoring starvation and recovery phases of
766 patients suffering from anorexia nervosa. *Rapid Communications in Mass*
767 *Spectrometry* 20(10), 1604-1610
768

769 Mellars, P.A., 2004. Reindeer specialization in the early Upper Palaeolithic: the
770 evidence from south west France. *Journal of Archaeological Science* 31(5), 613-617.
771

772 Murphy, B.P., Bowman, D.M., 2006. Kangaroo metabolism does not cause the
773 relationship between bone collagen $\delta^{15}\text{N}$ and water availability. *Functional*
774 *Ecology* 20(6), 1062-1069.
775

776 Newsome, S. D., Clementz, M. T., Koch, P. L., 2010. Using stable isotope
777 biogeochemistry to study marine mammal ecology. *Marine Mammal Science*, 26(3),
778 509–572.
779

780 Pardo L. H., Templer P. H., Goodale C. L., Duke S., Groffman P. M., Adams M. B., *et*
781 *al.* 2006. Regional assessment of N saturation using foliar and root
782 $\delta^{15}\text{N}$. *Biogeochemistry* 80, 143–171.
783

784 Park, R., Epstein, S., 1960. Carbon isotope fractionation during photosynthesis.
785 *Geochimica et Cosmochimica Acta* 21, 110-126.

786 Pederzani, S., Britton, K., 2019. Oxygen isotopes in bioarchaeology: Principles and
787 applications, challenges and opportunities. *Earth-science reviews* 188, 77-107.
788

789 Penkman, K.E.H., Preece, R.C., Bridgland, D.R., Keen, D.H., Meijer, T., Parfitt, S.A.
790 *et al.* 2011. A chronological framework for the British Quaternary based on Bithynia
791 opercula . *Nature* 476, 446-449.
792

793 Penkman, K.E.H., Preece, R.C., Bridgland, D.R., Keen, D.H., Meijer, T., Parfitt, S.A.
794 *et al.* 2013. An aminostratigraphy for the British Quaternary based on Bithynia
795 opercula. *Quaternary Science Reviews* 61, 111-134.
796

797 Podlesak, D.W., Torregrossa, A.M., Ehleringer, J.R., Dearing, M.D., Passey, B.H.,
798 Cerling, T.E., 2008. Turnover of oxygen and hydrogen isotopes in the body water,
799 CO₂, hair, and enamel of a small mammal. *Geochimica et Cosmochimica Acta* 72,
800 19-35.

801
802 Polischuk, S.C., Hobson, K.A., Ramsay, M.A., 2001. Use of stable-carbon and-
803 nitrogen isotopes to assess weaning and fasting in female polar bears and their
804 cubs. *Canadian Journal of Zoology* 79(3), 499-511.
805
806 Pryor, A.J., Stevens, R.E., O'Connell, T.C., Lister, J.R., 2014. Quantification and
807 propagation of errors when converting vertebrate biomineral oxygen isotope data to
808 temperature for palaeoclimate reconstruction. *Palaeogeography, palaeoclimatology,*
809 *palaeoecology* 412, 99-107.
810
811 Reade, H., O'Connell, T.C., Barker, G., Stevens, R.E., 2016. Pleistocene and
812 Holocene palaeoclimates in the Gebel Akhdar (Libya) estimated using herbivore
813 tooth enamel oxygen isotope compositions. *Quaternary International* 404, 150-162.
814
815 Reade, H., Tripp, J.A., Charlton, S., Grimm, S., Sayle, K.L., Fensome, A., Higham,
816 T.F., Barnes, I., Stevens, R.E., 2020a. Radiocarbon chronology and environmental
817 context of Last Glacial Maximum human occupation in Switzerland. *Scientific*
818 *Reports* 10(1), 4694.
819
820 Reade, H., Tripp, J.A., Charlton, S., Grimm, S., Leesch, D., Müller, W., Sayle, K.L.,
821 Fensome, A., Higham, T.F., Barnes, I., Stevens, R.E., 2020b. Deglacial landscapes
822 and the Late Upper Palaeolithic of Switzerland. *Quaternary Science Reviews* 239,
823 106372.
824
825 Richards, M.P., Taylor, G., Steele, T., McPherron, S.P., Soressi, M., Jaubert, J.,
826 Orschiedt, J., Mallye, J.B., Rendu, W., Hublin, J.J., 2008. Isotopic dietary analysis of
827 a Neanderthal and associated fauna from the site of Jonzac (Charente-Maritime),
828 France. *Journal of Human Evolution* 55, 179-185.
829
830 Rozanski, K.L., Araguás-Araguás, L., Conginatini, R., 1993. Isotopic Patterns in
831 Modern Global Precipitation. In: Swart, P.K., Lohmann, K.C., Mckenzie, J., Savin, S.
832 (Eds.), *Climate Change in Continental Isotopic Records*. Geophysical Monograph
833 Series Vol. 78, American Geophysical Union, Washington DC, pp. 1-36.
834
835 Schreve, D.C., 1997. Mammalian biostratigraphy of the later Middle Pleistocene in
836 Britain. Unpublished Doctoral thesis, University College London.
837

838 Sponheimer, M., Lee-Thorp, J.A., 2003. Using carbon isotope data of fossil bovid
839 communities for palaeoenvironmental reconstruction: research articles: human
840 origins research in South Africa. *South African Journal of Science* 99(5), 273-275.
841

842 Stevens, R.E., Hedges, R.E., 2004. Carbon and nitrogen stable isotope analysis of
843 northwest European horse bone and tooth collagen, 40,000 BP–present:
844 Palaeoclimatic interpretations. *Quaternary Science Reviews* 23(7-8), 977-991.
845

846 Stevens, R.E., Hermoso-Buxán, X.L., Marín-Arroyo, A.B., González-Morales, M.R.,
847 Straus, L.G., 2014. Investigation of Late Pleistocene and Early Holocene
848 palaeoenvironmental change at El Mirón cave (Cantabria, Spain): Insights from
849 carbon and nitrogen isotope analyses of red deer. *Palaeogeography,*
850 *Palaeoclimatology, Palaeoecology*, 414, 46-60.
851

852 Stevens, R.E., Jacobi, R., Street, M., Germonpré, M., Conard, N.J., Münzel, S.C. and
853 Hedges, R.E., 2008. Nitrogen isotope analyses of reindeer (*Rangifer tarandus*),
854 45,000 BP to 9,000 BP: Palaeoenvironmental reconstructions. *Palaeogeography,*
855 *Palaeoclimatology, Palaeoecology* 262(1-2), 32-45.
856

857 Stevens, R.E., O'Connell, T.C., Hedges, R.E., Street, M., 2009. Radiocarbon and
858 stable isotope investigations at the Central Rhineland sites of Gönnersdorf and
859 Andernach-Martinsberg, Germany. *Journal of Human Evolution* 57(2), 131-148.
860

861 Szpak, P., 2014. Complexities of nitrogen isotope biogeochemistry in plant-soil
862 systems: implications for the study of ancient agricultural and animal management
863 practices. *Frontiers in Plant Science* 5(288), 1-19.
864

865 Szpak, P., Gröcke, D.R., Debruyne, R., MacPhee, R.D., Guthrie, R.D., Froese, D.,
866 Zazula, G.D., Patterson, W.P., Poinar, H.N., 2010. Regional differences in bone
867 collagen $\delta^{13}\text{C}$ and $\delta^{15}\text{N}$ of Pleistocene mammoths: implications for paleoecology of
868 the mammoth steppe. *Palaeogeography, Palaeoclimatology, Palaeoecology* 286(1-
869 2), 88-96.
870

871 Tieszen, L.L., Fagre, T., 1993. Effect of diet quality and composition on the isotopic
872 composition of respiratory CO₂, bone collagen, bioapatite and soft tissues. In:
873 Lambert, J., Grupe, G. (Eds.), *Prehistoric Human Bone: Archaeology at the*
874 *Molecular Level*. Springer-Verlag, New York, 121-155.

875

876 Wißing, C., Rougier, H., Crevecoeur, I., Germonpré, M., Naito, Y.I., Semal, P.,
877 Bocherens, H., 2016. Isotopic evidence for dietary ecology of late Neandertals in
878 North-Western Europe. *Quaternary International* 411, 327-345.

879

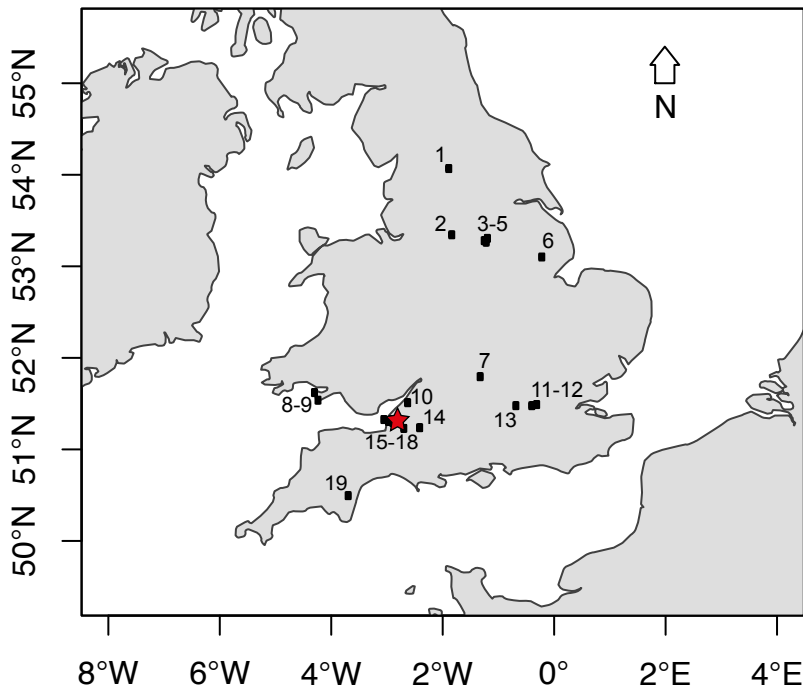
880 Zazzo, A., Lécuyer, C., Sheppard, S.M., Grandjean, P., Mariotti, A., 2004.

881 Diagenesis and the reconstruction of paleoenvironments: a method to restore original
882 $\delta^{18}\text{O}$ values of carbonate and phosphate from fossil tooth enamel. *Geochimica et*
883 *Cosmochimica Acta* 68(10), 2245-2258.

884

885 Figure 1: Sites in the British Isles containing a Banwell Bone Cave mammal
886 assemblage-zone fauna. Red star = Banwell Bone Cave; 1 Stump Cross Cave; 2
887 Windy Knoll Cave; 3 Steetley Wood Cave; 4 Ash Tree Cave; 5 The Arch (aka Lion's
888 Mouth); 6 Tattershall Castle; 7 Cassington; 8 Bosco's Den; 9 Port Eynon Point Cave;
889 10 Pen Park Quarry; 11 Kew Bridge Station; 12 Willment's Pit, Isleworth; 13 Windsor;
890 14 Limekiln Hill Quarry; 15 Brean Down; 16 Bleadon Quarry; 17 Picken's Hole; 18
891 Hyena Den; 19 Tornewton Cave. (After Current and Jacobi, 2001).

892

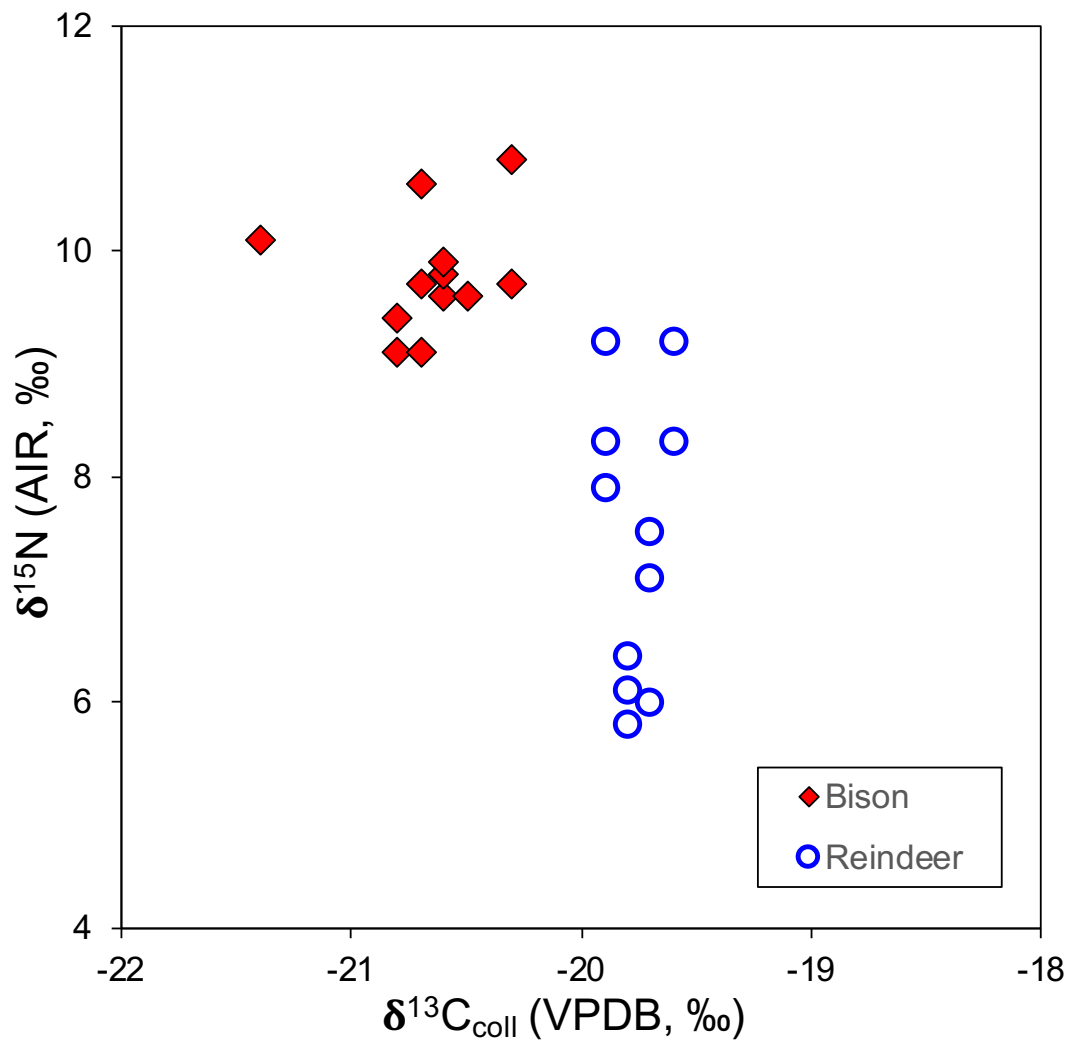


893

894

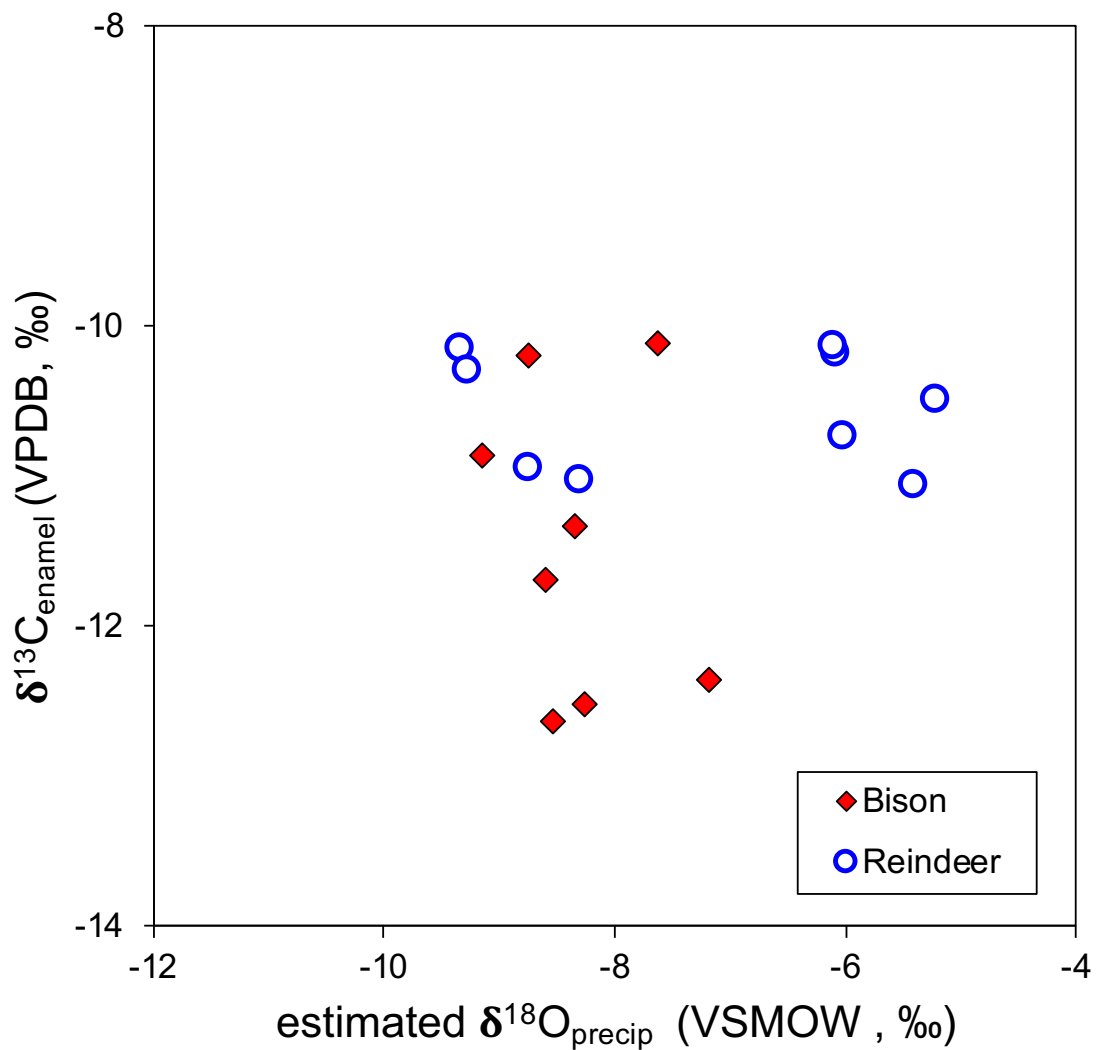
895

896 Figure 2: Banwell Bone Cave bison and reindeer bone collagen $\delta^{13}\text{C}$ and $\delta^{15}\text{N}$
897 results.
898



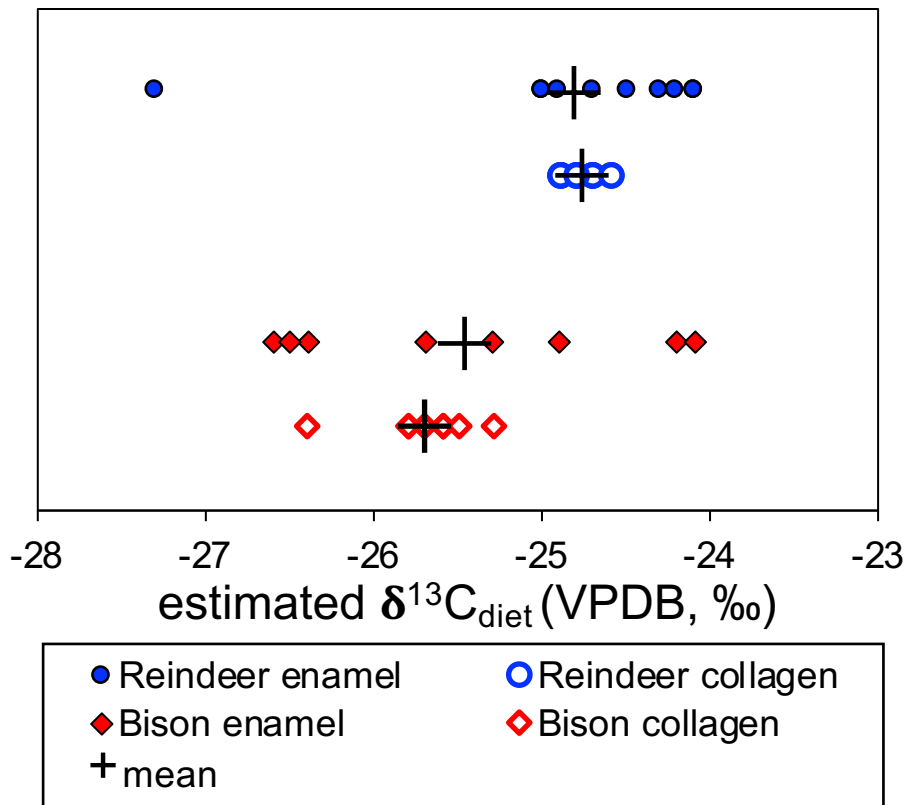
899
900
901

902 Figure 3: Bison and reindeer calculated drinking water $\delta^{18}\text{O}$ values plotted against
903 enamel $\delta^{13}\text{C}$ (See supplementary file 3 for enamel $\delta^{18}\text{O}$ values).
904



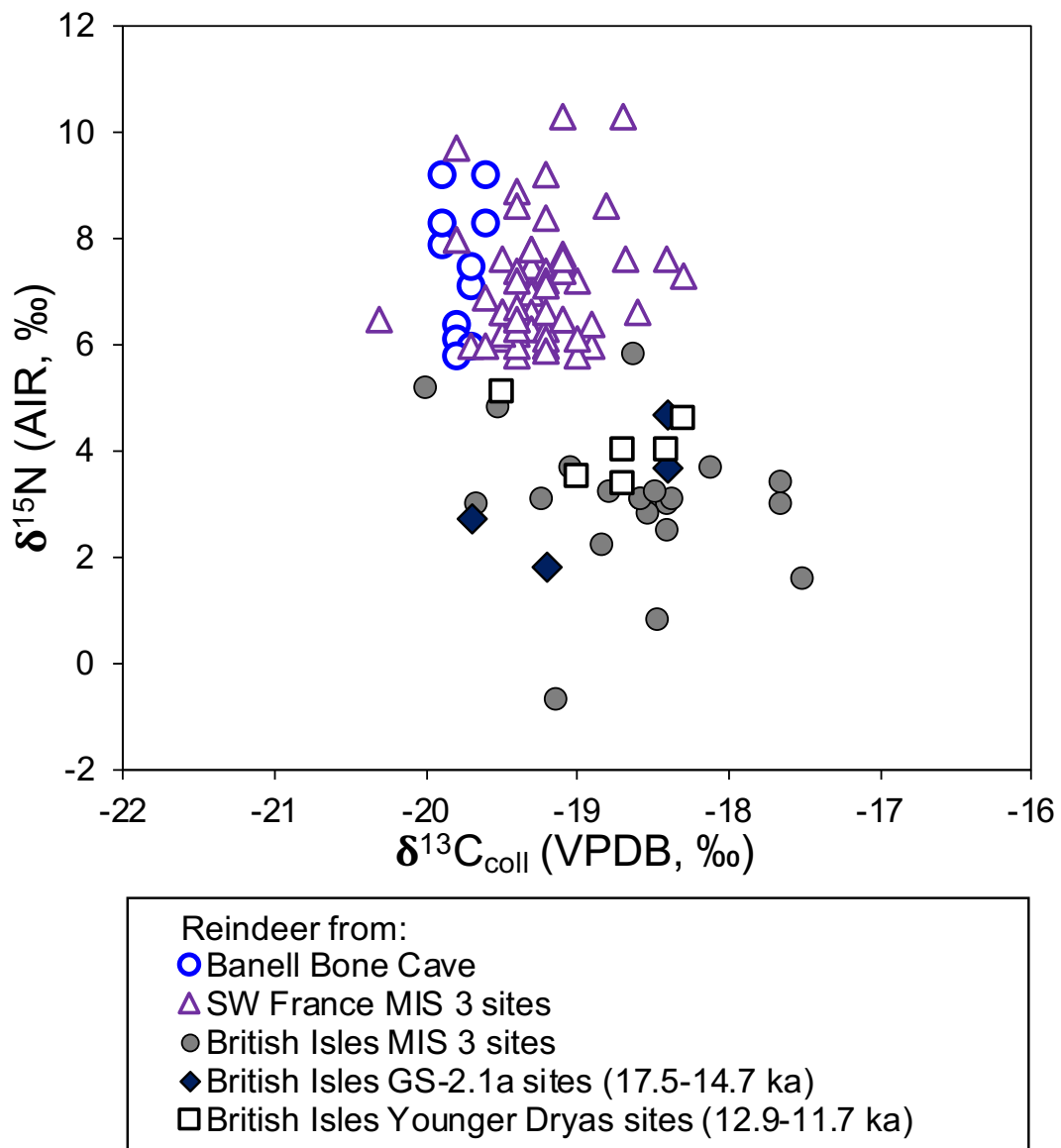
905
906
907

908 Figure 4: Calculated carbon isotope values of the diet consumed by Banwell Bone
909 Cave bison and reindeer.



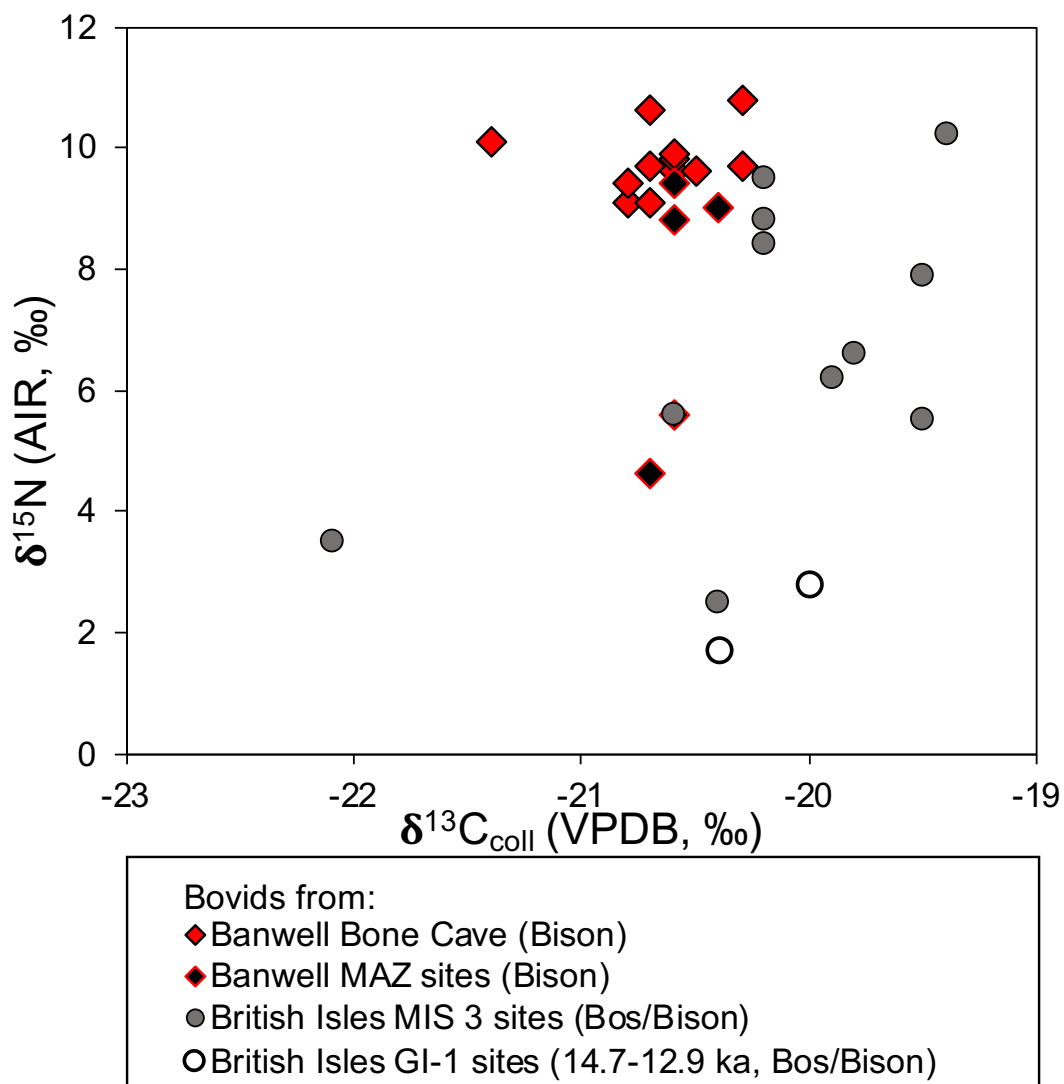
910
911
912

913 Figure 5: Bone collagen $\delta^{13}\text{C}$ and $\delta^{15}\text{N}$ of late Pleistocene reindeer from the UK and
914 southwest France. Additional data not produced for this publication has been collated
915 from the published literature (Full details are given in Supplementary file 4).



916
917

918 Figure 6: Bone collagen $\delta^{13}\text{C}$ and $\delta^{15}\text{N}$ of late Pleistocene Bovids from the UK and
919 southwest France. Additional data not produced for this publication has been collated
920 from the published literature (For full details see Supplementary file 5).
921



922
923
924
925
926

Supplementary text 1: ZooMS Methodology:

A recording error resulted in the failure to record the element used to identify select specimens to species. Due to Covid-19 restrictions preventing access to collections, the elements used to identify species could not be re-checked. To confirm initial species identifications collagen peptide fingerprints were obtained for these specimens. This was undertaken following methods adapted from Buckley et al. (2009) and Welker et al. (2015) using the acid-insoluble collagen. For each sample, around 100 ng of already extracted collagen were transferred to Eppendorf micro-tubes and gelatinised in 50 μ l 50 mM Ammonium Bicarbonate for 1h at 65°C. Samples were then incubated overnight at 37°C with 0.4 μ g of sequencing grade modified trypsin (Promega). Following trypsin digestion, samples were acidified with 0.5% trifluoroacetic acid (TFA) and purified using Pierce™ 100 μ l C18 resin Tips (Thermo Scientific) using conditioning and eluting solutions composed of 50% acetonitrile and 0.1% TFA. Collagen was eluted in 50 μ L.

For MALDI-TOF-MS, 0.5 μ L of the trypsin-digested extract was spotted with 0.5 μ L of α -cyano-hydroxycinnamic acid matrix solution (0.1% TFA in ACN/H₂O 1:1 v/v) onto a 48 spot MALDI target plate, and air dried. MALDI-MS analyses were carried out in triplicate on a Shimadzu MALDI 8020 instrument, operating at up to 2000 laser shots per plate spot, over a m/z range of 900-4000. The mass spectra were calibrated against an adjacent MS standard spot containing eight calibrant peptides (TOFMix™) of 0.8 to 3.7 kiloDalton (kDa) range (Bradykinin 1-7, angiotensin II, angiotensin I, Glu1-fibrinopeptide B, N-acetyl Renin substrate, ACTH 1–17 clip, ACTH 18–39 clip and ACTH 7–38 clip) – of which seven were used (1.0 – 3.7 kDa range).

The obtained collagen fingerprints were manually inspected for the presence of relevant peptide markers (A-G) in mMass v. 5.5.0 (Strohalm et al., 2010), after filtering peaks with a signal-to-noise ratio (S/N) threshold of 3.0 (Kirby et al., 2013), and using previously published collagen peptide markers from reference spectra (Buckley et al. 2009, 2017; Welker et al., 2016).

All initial species identifications were confirmed by ZooMs analysis (See table S1.1 and S1.2)

Table S1.1 ZooMS results. Columns P1 to G1 indicate identified peaks in the mass spectra. ZooMS identification is based on these peaks

Sample ID	P1	A	A'	B	C	P2	D	E	F	F'	G	G'	ZooMS ID
BW1	1105.2		1209.3	1427.4	1580.4	1648.5	2130.9		2853.1				<i>Bison / Bos sp</i>
BW8	1105.4	1192.5	1208.5	1427.7	1580.7	1648.8	2131.2	2792.8	2853.8			3035.1 - shifted by 1 amu	<i>Bison / Bos sp</i>
BW11	1105.3			1427.5	1580.5	1648.6	2130.9			2899.4		3094.7 - shifted by 1 amu	<i>Capra sp / Rangifer</i>
BW12	1105.6	1150.6	1196.4	1427.7	1580.8	1648.8	2131.1					3094.9 - shifted by 1 amu	<i>Rangifer</i>
BW13	1105.6		1166.6	1427.9	1581.0	1649.0	2131.4		2883.0				<i>Rangifer</i>
BW17	1105.5			1427.6	1580.6	1648.7	2130.9		2883.1			3093.0	<i>Capra sp / Rangifer</i>
BW19	1105.6		1166.6	1427.7	1580.8	1648.8	2131.0		2883.5			3093.7	<i>Rangifer</i>
BW20	1105.6	1150.6		1427.7	1580.7	1648.8	2131.0		2883.3			3093.9	<i>Rangifer</i>

Table S1.2 Most probable identification based on macroscopic zooarchaeological, ZooMS and stratigraphic context.

Sample ID	Macroscopic zooarchaeological identification	ZooMS identification	Most probable identification ¹
BW1	<i>Bison</i>	<i>Bison / Bos sp</i>	<i>Bison</i>
BW8	<i>Bison</i>	<i>Bison / Bos sp</i>	<i>Bison</i>
BW11	<i>Rangifer tarandus</i>	<i>Capra sp / Rangifer</i>	<i>Rangifer tarandus</i>
BW12	<i>Rangifer tarandus</i>	<i>Rangifer</i>	<i>Rangifer tarandus</i>
BW13	<i>Rangifer tarandus</i>	<i>Rangifer</i>	<i>Rangifer tarandus</i>
BW17	<i>Rangifer tarandus</i>	<i>Capra sp / Rangifer</i>	<i>Rangifer tarandus</i>
BW19	<i>Rangifer tarandus</i>	<i>Rangifer</i>	<i>Rangifer tarandus</i>
BW20	<i>Rangifer tarandus</i>	<i>Rangifer</i>	<i>Rangifer tarandus</i>

Supplementary text 1 bibliography:

Buckley, M., Collins, M., Thomas-Oates, J., Wilson, J.C., 2009. Species identification by analysis of bone collagen using matrix-assisted laser desorption/ionisation time-of-flight mass spectrometry. *Rapid Commun Mass Spectrom* 23 (23), 3843–3854.

Buckley, M., Harvey, V.L., Chamberlain, A.T., 2017. Species identification and decay assessment of Late Pleistocene fragmentary vertebrate remains from Pin Hole Cave (Creswell Crags, UK) using collagen fingerprinting. *Boreas* 46, 402–411.

Kirby, D.P., Buckley, M., Promise, E., Trauger, S., Holdcraft, T.R., 2013. Identification of collagen-based materials in cultural heritage. *Analyst* 138 (17), 4849–4858.

Strohalm, M., Kavan, D., Novak, P., Volny, M., Havlicek, V., 2010. mMass 3: a crossplatform software environment for precise analysis of mass spectrometric data. *Anal. Chem.* 82 (11), 4648–4651.

Welker, F., Soressi, M., Rendu, W., Hublin, J.-J., Collins, M.J., 2015. Using ZooMS to identify fragmentary bone from the Late Middle/Early Upper Palaeolithic sequence of Les Cottés, France. *J Archaeol Sci*, 54, 279–286.

Welker, F., Hajdinjak, M., Talamo, S., Jaouen, K., Dannemann, M., David, F., Julien M., Meyer, M., Kelso, J., Barnes, I., Brace, S., Kamminga, P., Fischer, R., Kessler, B.M., Stewart, J.R., Pääbo, S., Collins, M.J., Hublin, J.-J., 2016. Palaeoproteomic evidence identifies archaic hominins associated with the Châtelperronian at the Grotte du Renne. *PNAS*, 113 (40): 11162–11167.

Supplementary Table 1: Sample details and bone collagen carbon and nitrogen stable isotope results.

Sample code	Sample no	Find no	Species	Element	%C	%N	$\delta^{13}\text{C}$	$\delta^{15}\text{N}$	C:N	source
BW1	39	43	Bison	*	33.6	12.3	-20.6	9.6	3.2	1
BW2	10	11 (a)	Bison	Phalange	38.6	14.2	-20.8	9.1	3.2	1
BW3	21	23	Bison	Astragalus	42.6	15.6	-21.4	10.1	3.2	1
BW4	26	25	Bison	Vertebrae	41.8	15.3	-20.7	9.7	3.2	1
BW5	10	16	Bison	Phalange	40.4	14.8	-20.6	9.8	3.2	1
BW6	39	40	Bison	Scapula	43.5	15.9	-20.3	9.7	3.2	1
BW7	1	8	Bison	Phalange	43.3	15.8	-20.6	9.9	3.2	1
BW8	10	11	Bison	*	47.3	17.4	-20.7	9.1	3.2	1
BW9	45	47	Bison	Vertebrae	43.8	16	-20.5	9.6	3.2	1
BW10	8	1	Bison	Vertebrae	44.6	16.3	-20.8	9.4	3.2	1
OxA-14136			Bison	calcaneum	41.2		-20.3	10.8	3.2	2
OxA-14138			Bison	calcaneum	41.1		-20.7	10.6	3.1	2
BW11	10	12	Reindeer	*	43.5	15.8	-19.9	9.2	3.2	1
BW12	18	19	Reindeer	*	41.6	15.2	-19.8	6.4	3.2	1
BW13		7	Reindeer	*	40.3	14.7	-19.8	6.1	3.2	1
BW14	33	38	Reindeer	Vertebrae	41.9	15.3	-19.7	7.1	3.2	1
BW15		5	Reindeer	Mandible	40.9	14.9	-19.6	8.3	3.2	1
BW16	45	46	Reindeer	Maxilla	42.3	15.4	-19.7	7.5	3.2	1
BW17	18	17	Reindeer	*	42.8	15.7	-19.7	6	3.2	1
BW18		14	Reindeer	Astragalus	46.3	17	-19.9	7.9	3.2	1
BW19	21	24	Reindeer	*	52.5	19.2	-19.9	8.3	3.2	1
BW20	60	61	Reindeer	*	49.5	18.1	-19.6	9.2	3.2	1
BW21	33	36	Reindeer	Scapula	43.3	15.8	-19.8	5.8	3.2	1

1: This study

2: Higham, T. G., Jacobi, R. M. & Bronk Ramsey, C. AMS radiocarbon dating of ancient bone using ultrafiltration. Radiocarbon 48, 179–195 (2006)

* Element not recorded so species identification was confirmed by ZooMs. See supplementary text 1

Supplementary Table 2: Sample details, tooth enamel oxygen and carbon isotope results, and results of conversion equations

Sample code	Species	Notes	Tooth	Animal age during formation (months)	Measured enamel carbonate $\delta^{13}\text{C}$	Measured enamel carbonate $\delta^{18}\text{O}$ vpdb	Calculated carbonate $\delta^{18}\text{O}$ vsmow (equation 1)	Calculated phosphate $\delta^{18}\text{O}$ vsmow (equation 2)	Calculated drinking water $\delta^{18}\text{O}$ vsmow (bison equation 3, reindeer equation 4)
ED1	Bison		Upper left P3/P4	9 months to c.30months	-10.9	-7.0	23.7	14.9	-9.1 ± 2.6
ED2	Bison		Upper left M1/M2	en utero to c.13 months	-12.6	-6.6	24.1	15.3	-8.5 ± 2.7
ED3	Bison		Lower right P3/P4	9 months to c.30months	-11.7	-6.7	24.0	15.3	-8.6 ± 2.6
ED4	Bison		Upper left M1/M2	en utero to c.13 months	-12.4	-5.7	25.0	16.2	-7.1 ± 2.7
ED5	Bison		Upper left M1/M2	en utero to c.13 months	-11.3	-6.5	24.2	15.5	-8.3 ± 2.7
ED11	Bison		Lower M1	en utero to c.4months	-12.5	-6.4	24.3	15.5	-8.2 ± 2.7
ED12	Bison		Upper left M3	9 months to c.24months	-10.2	-6.8	23.9	15.2	-8.7 ± 2.6
ED13	Bison		Upper Left M2	Birth to c.13 months	-10.1	-6.0	24.7	15.9	-7.6 ± 2.7
ED14	Reindeer		Lower Left M1/M2	3 to 9 months	-11	-5.1	25.6	16.8	-4.8 ± 2.8
ED15	Reindeer		Lower Left M1/M2	3 to 9 months	-10.1	-8.2	22.5	13.8	-9.3 ± 2.4
ED16	Reindeer	ED16, ED23 from same mandible	Left lower P2	13 to 18 months	-10.5	-5.0	25.8	17.0	-4.6 ± 2.8
ED17	Reindeer		Upper Left P2/dp2?	13 to 18 months	-13.3	-8.0	22.6	13.9	-9.1 ± 2.4
ED18	Reindeer		Upper right M3	9 to 26 months	-10.7	-5.6	25.1	16.3	-5.5 ± 2.7
ED19	Reindeer	ED19, ED20 from same mandible	Upper Left M3	9 to 26 months	-10.2	-5.6	25.1	16.3	-5.6 ± 2.7
ED20	Reindeer	ED19, ED20 from same mandible	Upper Left M2	13 to 18 months	-10.3	-8.1	22.5	13.8	-9.2 ± 2.4
ED21	Reindeer	ED21, ED22 from same mandible	Lower left P3	13 to 18 months	-11	-7.4	23.3	14.6	-8.1 ± 2.5
ED22	Reindeer	ED21, ED22 from same mandible	Lower Left P2	13 to 18 months	-10.9	-7.7	23.0	14.2	-8.6 ± 2.4
ED23	Reindeer	ED16, ED23 from same mandible	Left lower P3	13 to 18 months	-10.1	-5.7	25.1	16.3	-5.6 ± 2.7
Bison-based palaeo- $\delta^{18}\text{O}$ precip estimate									-8.3 ± 1.3
Reindeer-based palaeo- $\delta^{18}\text{O}$ precip estimate									-7.0 ± 1.6
Bison-based temperature estimate (°C) (equation 5)									10.3 ± 2.5
Reindeer-based temperature estimate (°C) (equation 5)									12.8 ± 3.1

Equation 1: $\delta^{18}\text{O}_{\text{VSMOW}} = 1.03091 * \delta^{18}\text{O}_{\text{VPDB}} + 30.91$ (Coplen 2011)

Equation 2: $\delta^{18}\text{O}_{\text{phos}} = 0.973 * \delta^{18}\text{O}_{\text{carb}} - 8.12$ (Zazzo et al. 2004)

Equation 3: $\delta^{18}\text{O}_{\text{envi}} = (\delta^{18}\text{O}_{\text{carb}} - 30.057 (\pm 0.58)) / 0.703 (\pm 0.12)$ (based on Hoppe 2006)

Equation 4: $\delta^{18}\text{O}_{\text{envi}} = (\delta^{18}\text{O}_{\text{phos}} - 20.117 (\pm 0.34)) / 0.683 (\pm 0.11)$ (based on Longinelli et al., 2003)

Equation 5: temperature (°C) = $(\delta^{18}\text{O}_{\text{precip}} - 13.74 (\pm 0.16)) / 0.53 (\pm 0.08)$ (Pryor et al., 2014)

Timing of crown formation or enamel mineralization in Rangifer is estimated here based on known information for other deer species as this information is yet to be established for reindeer (Brown and Chapman, 1991a, b).

For Bison, these estimates are based on Gadbury et al. 2000.

Supplementary table 2 bibliography

- Coplen, T. B., 2011. Guidelines and recommended terms for expression of stable-isotope-ratio and gas-ratio measurement results. *Rapid Communications in Mass Spectrometry* 25(17), 2538–2560.
- Zazzo, A., Lécuyer, C., Sheppard, S.M., Grandjean, P., Mariotti, A., 2004. Diagenesis and the reconstruction of paleoenvironments: a method to restore original $\delta^{18}\text{O}$ values of carbonate and phosphate from fossil tooth enamel. *Geochimica et Cosmochimica Acta* 68(10), 2245-2258.
- Hoppe, K.A. 2006. Correlation between the oxygen isotope ratio of North American bison teeth and local waters: implication for paleoclimatic reconstructions. *Earth Planetary Science Letters* 244 (1-2), 408-417.
- Longinelli, A., Iacumin, P., Davanzo, S., Nikolaev, V., 2003. Modern reindeer and mice: revised phosphate–water isotope equations. *Earth and Planetary Science Letters* 214(3-4), 491-498.
- Pryor, A.J., Stevens, R.E., O'Connell, T.C., Lister, J.R., 2014. Quantification and propagation of errors when converting vertebrate biomineral oxygen isotope data to temperature for palaeoclimate reconstruction. *Palaeogeography, Palaeoclimatology, Palaeoecology* 412, 99-107.
- Brown, W.A.B., Chapman, N.G., 1991a. Age assessment of fallow deer (*Dama dama*) from a scoring scheme based on radiographs of developing permanent molariform teeth. *Journal of Zoology* 224(3), 367-379.
- Brown, W.A.B., Chapman, N.G., 1991b. The dentition of red deer (*Cervus elaphus*): a scoring scheme to assess age from wear of the permanent molariform teeth. *Journal of Zoology* 224(4), 519-536.
- Gadbury, C., Todd, L., Jahren, A.H., Amundson, R., 2000. Spatial and temporal variations in the isotopic composition of bison tooth enamel from the Early Holocene Hudson-Meng Bone Bed, Nebraska. *Palaeogeography, Palaeoclimatology, Palaeoecology* 157 (1-2), 79-93.

Supplementary Table 3: Results of conversion of collagen and carbonate $\delta^{13}\text{C}$ data to estimated $\delta^{13}\text{C}$ diet.

Sample code	Species	$\delta^{13}\text{C}$	Material	Calculated $\delta^{13}\text{C}$ diet
BW1	Bison	-20.6	Collagen	-25.6
BW2	Bison	-20.8	Collagen	-25.8
BW3	Bison	-21.4	Collagen	-26.4
BW4	Bison	-20.7	Collagen	-25.7
BW5	Bison	-20.6	Collagen	-25.6
BW6	Bison	-20.3	Collagen	-25.3
BW7	Bison	-20.6	Collagen	-25.6
BW8	Bison	-20.7	Collagen	-25.7
BW9	Bison	-20.5	Collagen	-25.5
BW10	Bison	-20.8	Collagen	-25.8
OxA-14136	Bison	-20.3	Collagen	-25.3
OxA-14138	Bison	-20.7	Collagen	-25.7
BW11	Reindeer	-19.9	Collagen	-24.9
BW12	Reindeer	-19.8	Collagen	-24.8
BW13	Reindeer	-19.8	Collagen	-24.8
BW14	Reindeer	-19.7	Collagen	-24.7
BW15	Reindeer	-19.6	Collagen	-24.6
BW16	Reindeer	-19.7	Collagen	-24.7
BW17	Reindeer	-19.7	Collagen	-24.7
BW18	Reindeer	-19.9	Collagen	-24.9
BW19	Reindeer	-19.9	Collagen	-24.9
BW20	Reindeer	-19.6	Collagen	-24.6
BW21	Reindeer	-19.8	Collagen	-24.8
ED1	Bison	-10.9	Enamel	-24.9
ED2	Bison	-12.6	Enamel	-26.6
ED3	Bison	-11.7	Enamel	-25.7
ED4	Bison	-12.4	Enamel	-26.4
ED5	Bison	-11.3	Enamel	-25.3
ED11	Bison	-12.5	Enamel	-26.5
ED12	Bison	-10.2	Enamel	-24.2
ED13	Bison	-10.1	Enamel	-24.1
ED14	Reindeer	-11	Enamel	-25
ED15	Reindeer	-10.1	Enamel	-24.1
ED16	Reindeer	-10.5	Enamel	-24.5
ED17	Reindeer	-13.3	Enamel	-27.3
ED18	Reindeer	-10.7	Enamel	-24.7
ED19	Reindeer	-10.2	Enamel	-24.2
ED20	Reindeer	-10.3	Enamel	-24.3
ED21	Reindeer	-11	Enamel	-25
ED22	Reindeer	-10.9	Enamel	-24.9
ED23	Reindeer	-10.1	Enamel	-24.1

$\delta^{13}\text{C}_{\text{coll}}$ and $\delta^{13}\text{C}_{\text{enamel}}$ were converted to $\delta^{13}\text{C}_{\text{diet}}$ by assuming a diet to collagen offset of +5‰, and diet to carbonate offset of +14‰ following Lee Thorpe *et al.* 1989 and Cerling and Harris 1999

Lee-Thorp, J. A., Sealy, J. C., van der Merwe, N. J., 1989. Stable carbon isotope ratio differences between bone collagen and bone apatite and their relationship to diet. *Journal of Archaeological Science* 16(6), 585-599.

Cerling, T. E., Harris, J. M., 1999. Carbon isotope fractionation between diet and bioapatite in ungulate mammals and implications for ecological and paleoecological studies. *Oecologia* 120(3), 347-363.

Supplementary Table 4: Bone collagen $\delta^{13}\text{C}$ and $\delta^{15}\text{N}$ of late Pleistocene reindeer from the UK and southwest France collated from published literature.

Site Name	Country	Element	Lab code	Direct ^{14}C date lab Code	Direct ^{14}C date	uncertainty on ^{14}C date	Age category	Collagen $\delta^{13}\text{C}$	Collagen $\delta^{15}\text{N}$	Collagen C:N ratio	Date reference	Carbon (coll) reference	Nitrogen (coll) reference
Sun Hole Cave	UK	1st phalange	OxA-14827	OxA-14827	10145	55	GS-1 (Younger Dryas)	-18.3	4.6	3.2	11	11	11
Kent's Cavern	UK	1st phalange	OxA-14825	OxA-14825	10255	45	GS-1 (Younger Dryas)	-19.5	5.1	3.2	11	11	11
Chelm's Combe	UK	left dentary	A/CC/B/6	OxA-17831	10480	45	GS-1 (Younger Dryas)	-18.4	4	3.2	11	11	11
Foxhole Cave	UK	astragalus	OxA-8312	OxA-8312	10685	65	GS-1 (Younger Dryas)	-18.7	3.4	3.3	15	15	15
Foxhole Cave	UK	astragalus	OxA-25145	OxA-25145	10780	50	GS-1 (Younger Dryas)	-19	3.5	3.2	16	16	16
Foxhole Cave	UK	tibia	OxA-8311	OxA-8311	10785	65	GS-1 (Younger Dryas)	-18.7	4	3.4	15	15	15
Gough's Cave	UK	antler	OxA-18064	OxA-18064	12535	55	GS-2.1a	-19.2	1.8	3.2	11	11	11
Foxhole Cave	UK	astragalus	OxA-25146	OxA-25146	12555	55	GS-2.1a	-19.7	2.7	3.2	16	16	16
Kent's Cavern	UK	astragalus, left	OxA-14826	OxA-14826	14395	60	GS-2.1a	-18.4	4.7	3.2	11	11	11
Reindeer Rift, Cattedown	UK	calcaneum, sin.	OxA-17160	OxA-17160	14550	55	GS-2.1a	-18.4	3.7	3.2	11	11	11
Goat's Hole (Paviland)	UK	bone	OxA-17560	OxA-17560	24240	110	OIS3	-17.7	3.4	3.3	12	12	12
Pontnewydd Cave	UK	1st phalange	OxA-13984	OxA-13984	25210	120	OIS3	-18.4	3.1	3.2	3	3	3
Goat's Hole (Paviland)	UK	antler	OxA-7084	OxA-7084	28550	650	OIS3	-19.2	3.1	3.1	15	15	15
Pontnewydd Cave	UK	metacarpal	OxA-13993	OxA-13993	30240	230	OIS3	-18.5	3.2	3.2	3	3	3
Pontnewydd Cave	UK	tibia	OxA-11672	OxA-11672	31800	1000	OIS3	-17.7	3	3.3	3	3	3
Goat's Hole (Paviland)	UK	antler	OxA-13438	OxA-13438	31990	180	OIS3	-19	3.7	3.2	12	12	12
Kent's Cavern	UK	antler	OxA-30162	OxA-30162	34850	600	OIS3	-18.8	3.2	3.4	14	14	14
Kent's Cavern	UK	antler	OxA-30272	OxA-30272	35100	650	OIS3	-19.1	-0.7	3.3	14	14	14
Pontnewydd Cave	UK	tibia	OxA-11671	OxA-11671	35400	>	OIS3	-19.7	3	3.4	3	3	3
Pontnewydd Cave	UK	humerus (left)	OxA-11669	OxA-11669	36700	>	OIS3	-20	5.2	3.5	3	3	3
Goat's Hole (Paviland)	UK	antler	OxA-13658	OxA-13658	37350	320	OIS3	-18.6	5.8	3.2	12	12	12
Pin Hole	UK	antler	OxA-11980	OxA-11980	37760	340	OIS3	-19.5	4.8	3.3	13	13	13
Pontnewydd Cave	UK	right mandible	OxA-14052	OxA-14052	39600	900	OIS3	-18.6	3.1	3.4	3	3	3
Kent's Cavern	UK	left dentary	OxA-13888	OxA-13888	40000	700	OIS3	-18.5	2.8	3.3	8	8	8
Pontnewydd Cave	UK	humerus (right)	OxA-11670	OxA-11670	40200	>	OIS3	-18.4	2.5	3.3	3	3	3
Goat's Hole (Paviland)	UK	antler	OxA-13439	OxA-13439	40570	370	OIS3	-18.8	2.2	3.2	12	12	12

Site Name	Country	Element	Lab code	Direct ¹⁴ C date lab Code	Direct ¹⁴ C date	uncertainty on ¹⁴ C date	Age category	Collagen δ ¹³ C	Collagen δ ¹⁵ N	Collagen C:N ratio	Date reference	Carbon (coll) reference	Nitrogen (coll) reference
Pin Hole	UK	antler	OxA-11797	OxA-11797	40650	500	OIS3	-18.5	0.8	3.4	8	8	8
Pontnewydd Cave	UK	astragalus	OxA-14055	OxA-14055	41400	1400	OIS3	-18.4	3	3.3	3	3	3
Pin Hole	UK	antler	OxA- 11796	OxA-11796	44200	800	OIS3	-17.5	1.6	3.3	8	8	8
Robin Hood's Cave	UK	bone	OxA-12772	OxA-12772	47300	1200	OIS3	-18.1	3.7	3.2	13	13	13
Kent's Cavern	UK	proximal radius	OxA-14714	OxA-14714	49600	2200	OIS3	-18.6	3.1	3.3	8	8	8
Abri Castanet	France	tibia	CST400	GifA 97312	32460	420	OIS 3	-19.5	7.6	3	2	2	2
Abri Castanet	France	metatarsus	CST600	GifA 97313	32750	460	OIS 3	-19.8	9.7	3.1	2	2	2
Abri Castanet	France	humerus	CST500	GifA 99165	31430	390	OIS 3	-19.2	9.2	3.1	2	2	2
Abri Castanet	France	tibia	CST300	GifA 99166	34320	520	OIS 3	-19.1	10.3	3.2	2	2	2
Abri Castanet	France	femur	CST200	GifA 99180	32950	520	OIS 3	-18.7	10.3	3	2	2	2
Abri Castanet	France	metatarsus	CST100				OIS 3	-18.8	8.6	3	2	2	2
Abri Castanet	France	humerus	CST-A1				OIS 3	-19.3	7.8	3.5	2	2	2
Abri Lartet	France	astragalus	LRT-2				OIS 3	-19.2	8.4	3.3	2	2	2
Abri Lartet	France	astragalus	LRT-3				OIS 3	-19.3	7.5	3.3	2	2	2
Abri Pasquet	France	calcaneum	PSQ-1				OIS 3	-19.4	8.9	3.5	2	2	2
Abri Pataud	France	Tibia	P-19918	OxA-21581	33550	550	OIS 3	-19.3	7.5	3.3	9	6	6
Abri Pataud	France	Metacarpal III-I	P-19931	OxA-21587	28150	290	OIS 3	-19.2	6	3.3	9	6	6
Abri Pataud	France	Central + fourth t	P-19932	OxA-21588	28250	280	OIS 3	-19.2	6	3.3	9	6	6
Abri Pataud	France	Tibia	P-19912	OxA-21599	34850	600	OIS 3	-18.6	6.6	3.3	9	6	6
Abri Pataud	France	Metatarsal III-I	P-19913	OxA-21600	34200	550	OIS 3	-19.2	7.4	3.3	9	6	6
Abri Pataud	France	Bone	P-21953	OxA-21670	33450	500	OIS 3	-19.2	7.2	3.4	9	6	6
Abri Pataud	France	Bone	P-21954	OxA-21671	34300	600	OIS 3	-19.1	7.5	3.3	9	6	6
Grotte XVI	France	metatarsus	G16-47				OIS 3	-19.1	7.7	3.3	2	2	2
Grotte XVI	France	metatarsus	G16-50				OIS 3	-19.3	7	3.2	2	2	2
Grotte XVI	France	tibia	G16-100				OIS 3	-19.3	6.6	3.3	2	2	2
Grotte XVI	France	mandible	G16-19				OIS 3	-19.5	6.1	3.4	2	2	2
Grotte XVI	France	radioulna	G16-20				OIS 3	-18.9	6	3.3	2	2	2
Grotte XVI	France	metatarsus	G16-23				OIS 3	-19	7.2	3.2	2	2	2
Grotte XVI	France	metatarsus	G16-24				OIS 3	-19.5	6.6	3.3	2	2	2

Site Name	Country	Element	Lab code	Direct ¹⁴ C date lab Code	Direct ¹⁴ C date	uncertainty on ¹⁴ C date	Age category	Collagen $\delta^{13}\text{C}$	Collagen $\delta^{15}\text{N}$	Collagen C:N ratio	Date reference	Carbon (coll) reference	Nitrogen (coll) reference
Grotte XVI	France	metacarpum	G16-25				OIS 3	-19.1	7.4	3.3	2	2	2
Grotte XVI	France	metatarsus	G16-26				OIS 3	-19.1	6.5	3.3	2	2	2
Grotte XVI	France	mandible	G16-37				OIS 3	-18.9	6.4	3.3	2	2	2
Grotte XVI	France	phalanx I	G16-70				OIS 3	-19	5.8	3.3	2	2	2
Grotte XVI	France	astragalus	G16-76				OIS 3	-19.8	8	3.3	2	2	2
Grotte XVI	France	metapodial	G16-93				OIS 3	-19.2	7.1	3.3	2	2	2
Grotte XVI	France	metacarpum	G16-94				OIS 3	-19.3	7.8	3.3	2	2	2
Grotte XVI	France	metacarpum	G16-95				OIS 3	-19.4	7.4	3.3	2	2	2
La Berbie	France	jawbone	LBR1100				OIS 3	-19.1	7.6	3.2	1	1	1
La Berbie	France	femur	LBR3400				OIS 3	-19.4	5.8	3.3	1	1	1
La Moustier	France	metacarpal	OxA-25170	OxA-25170	50000	3900	OIS 3	-19.4	6.2	3.5	10	10	10
La Quina	France	bone	OxA-21807	OxA-21807	45200	2200	OIS 3	-18.678	7.6	3.3	10	10	10
Le Moustier	France	calcaneum	G16-77				OIS 3	-19.3	6.3	3.3	2	2	2
Le Moustier	France	scapula	MST-12				OIS 3	-19.3	6.3	3.3	2	2	2
Les Peyrugues	France	humerus	PRG3900				OIS 3	-19.2	6.3	3.3	5	5	5
Les Peyrugues	France	radius	PRG5400				OIS 3	-19.4	6	3.1	5	5	5
Les Peyrugues	France	long bone	PRG5500				OIS 3	-19	6.1	3.3	5	5	5
Les Peyrugues	France	metatarsal	PRG5600				OIS 3	-19.7	6	3.2	5	5	5
Les Peyrugues	France	radius	PRG5800				OIS 3	-19.2	6.1	3.2	5	5	5
Les Pradelles / Marillac	France	bone	not given				OIS 3	-20.3	6.5	not given	7	7	7
Les Pradelles / Marillac	France	bone	not given				OIS 3	-19.6	6.9	not given	7	7	7
Les Pradelles / Marillac	France	bone	not given				OIS 3	-19.5	6.2	not given	7	7	7
Les Pradelles / Marillac	France	bone	not given				OIS 3	-19.4	6.5	not given	7	7	7
Les Pradelles / Marillac	France	bone	not given				OIS 3	-19.4	6.3	not given	7	7	7
Les Pradelles / Marillac	France	bone	not given				OIS 3	-19.2	5.9	not given	7	7	7
Les Pradelles / Marillac	France	bone	not given				OIS 3	-19.2	6.6	not given	7	7	7
Mandrin	France	femur	OxA-21694	OxA-21694	47100	0	OIS 3	-19.5	6.6	3.4	10	10	10
Roc-de-Combe	France	metatarsus	RCM-22				OIS 3	-18.4	7.6	3.3	2	2	2

Site Name	Country	Element	Lab code	Direct ¹⁴ C date lab Code	Direct ¹⁴ C date	uncertainty on ¹⁴ C date	Age category	Collagen δ ¹³ C	Collagen δ ¹⁵ N	Collagen C:N ratio	Date reference	Carbon (coll) reference	Nitrogen (coll) reference
Roc-de-Combe	France	metatarsus	RCM-23				OIS 3	-19.4	8.6	3.3	2	2	2
Roc-de-Combe	France	metatarsus	RCM-24				OIS 3	-19.1	6.5	3.2	2	2	2
Roc-de-Combe	France	phalanx	RCM-25				OIS 3	-19.8	8	3.3	2	2	2
Roc-de-Combe	France	maxillary	RCM-26				OIS 3	-19.4	7.2	3.3	2	2	2
Saint-Césaire	France	metapodium	RPB7200				OIS 3	-18.3	7.3	3.2	1	1	1
Saint-Césaire	France	not given	RPB3100				OIS 3	-19.4	6.7	3.2	4	4	4
Saint-Césaire	France	not given	RPB3700				OIS 3	-19.4	6.5	3.2	4	4	4
Vergisson II	France	bone	OxA-7758	OxA-7758	35700	2400	OIS 3	-19.604	6	3	17	18	17

Supplementary table 4 bibliography

1: Bocherens, H., Drucker, D.G., Billiou, D., Patou-Mathis, M., Vandermeersch, B. 2005. Isotopic evidence for diet and subsistence pattern of the Saint-Césaire I Neanderthal: Review and use of a multi-source mixing model. *Journal of Human Evolution* 49: 71–87.

2: Bocherens, H., Drucker, D.G., Madelaine, S., 2014. Evidence for a ¹⁵N positive excursion in terrestrial foodwebs at the Middle to Upper Palaeolithic transition in south-western France: implications for early modern humans. *Journal of Human Evolution* 69, 31-43.

3: Debenham, N.C., Pettitt, P.B., Housley, R.A., Higham, T.F.G., Rowe, N.P., Atkinson, T., Hebden, N. 2012. Neanderthals in Wales: Pontnewydd and the Elwy Valley. ed. / S.H.R. Aldhouse-Green; Rick Peterson; K.E. Walker. Cardiff : Oxbow Books in association with The National Museum of Wales, 302-320.

4: Drucker, D., Bocherens, H., Mariotti, A., Lévêque, F., Vandermeersch, B., Guadelli, J.-L., 1999. Conservation des signatures isotopiques du collagène d'os et de dents du Pléistocène supérieur (Saint-Césaire, France) : implications pour les reconstitutions des régimes alimentaires des néandertaliens. *Bulletins et Mémoires de la Société d'Anthropologie de Paris, Nouvelle Série, tome 11 fascicule 3-4*, pp. 289-305.

5: Drucker, D., Bocherens, H., Billiou, D. 2003. Evidence for shifting environmental conditions in Southwestern France from 33 000 to 15 000 years ago derived from carbon-13 and nitrogen-15 abundances in collagen of large herbivores. *Earth Planetary Science Letter* 216, 163–173.

6: Drucker, D.G., Vercoeur, C., Chiotti, L., Nespole, R., Crepin, L., Condard, N.J., Munzel, S.C., Higham, T., Plicht, J., Laznickova-Galetova, M. and Bocherens, H. 2015 Tracking possible decline of woolly mammoth during the Gravettian in Dordogne (France) and the Ach Valley (Germany) using multi-isotope tracking (13C, 14C, 15N, 34S, 18O). *Quaternary International*, 359, 304-317.

7: Fizet, M., Mariotti, A., Bocherens, H., 1995. Effect of Diet, Physiology and Climate on Carbon and Nitrogen Stable Isotopes of Collagen in a Late Pleistocene anthropic palaeoecosystem: Marillac, Charente, France. *Journal of Archaeological Science* 22(1), 67-79.

8: Higham, T.G., Jacobi, R.M., Bronk Ramsey, C., 2006. AMS radiocarbon dating of ancient bone using ultrafiltration. *Radiocarbon* 48(2), 179–195.

9: Higham, T., Jacobi, R., Basell, L., Bronk Ramsey, C., Chiotti, L., Nespoulet, R. 2011. Precision dating of the Palaeolithic: A new radiocarbon chronology for the Abri Pataud (France), a key Aurignacian sequence. *Journal of human evolution*, 61(5) 549-563.

10: Higham T, Douka K, Wood R, Ramsey CB, Brock F, Basell L, et al. The timing and spatiotemporal patterning of Neanderthal disappearance. *Nature*. 2014; 512: 306–309.

11: Jacobi, RM, Higham T. 2009. The early Late glacial re-colonization of Britain: new radiocarbon evidence from Gough's Cave, southwest England. *Quaternary Science Reviews*, 28 : 1895-1913

12: Jacobi, R.M., Higham, T.F.G. 2008. The 'Red Lady' ages gracefully: new ultrafiltration AMS determinations from Paviland. *Journal of Human Evolution*, 55: 898-907.

13: Jacobi, R.M., Higham, T.F.G., Bronk Ramsey, C. 2006. AMS radiocarbon dating of Middle and Upper Palaeolithic bone in the British Isles: improved reliability using ultrafiltration. *Journal of Quaternary Science*. 21 (5): 557–573.

- 14: Proctor, C., Douka, K., Proctor, J.W. and Higham, T. 2017. The Age and Context of the KC4 Maxilla, Kent's Cavern, UK. *European Journal of Archaeology* 20 (1) 2017, 74–97.
- 15: Richards, M. P. 2000. Human and faunal stable isotope analyses from Goat's Hole and Foxhole caves, Gower. Pp. 71-75 in S. Aldhouse-Green (ed.), *Paviland Cave and the "Red Lady": a definitive report*. Western Academic and Specialist Press, Ltd.: Bristol.
- 16: Schulting, R.J., Fibiger, L., Macphail, R.I., McLaughlin, R., Murray, E.V., Price, C., Walker, E.A. 2013a. Mesolithic and Neolithic humans remains from Foxhole Cave (Gower, South Wales). *Antiquaries Journal* 93: 1-23.
- 17: Stevens, R.E. Jacobi, R., Street, M., Germonpré, M., Conard, N.J., Münzel, S.C. Hedges, R.E.M. 2008 Nitrogen isotope analyses of reindeer (*Rangifer tarandus*), 45,000 BP to 9,000 BP: Palaeoenvironmental reconstructions. *Palaeogeography, Palaeoclimatology, Palaeoecology*, 262 (1-2) pp. 32-45.
- 18: ORAU database: <https://c14.arch.ox.ac.uk/database/db.php?page=checkDate&oxa=7758&auto=true>

Supplementary Table 5: Bone collagen $\delta^{13}\text{C}$ and $\delta^{15}\text{N}$ of late Pleistocene Bovids from the UK and southwest France collated from published literature.

Site Name	Country	Species	Element	Lab code	Direct ^{14}C date Lab Code	Direct ^{14}C date	Age category	Collagen $\delta^{13}\text{C}$	Collagen $\delta^{15}\text{N}$	Collagen C:N ratio	Date reference	Carbon (coll) reference	Nitrogen (coll) reference
Ash Tree Cave	UK	Bison priscus	cervical vertebra	OxA-15003	57700	>	Banwell MAZ site	-20.6	5.6	3.2	1	1	1
Windy Knoll	UK	Bison priscus	radius	OxA-15001	51700	>	Banwell MAZ site	-20.7	4.6	3.2	1	1	1
Steetley Quarry	UK	Bison priscus	metacarpal	OxA-15000	53200	>	Banwell MAZ site	-20.6	9.4	3.2	1	1	1
Ash Tree Cave	UK	Bison priscus	metatarsal	OxA-13800	54100	>	Banwell MAZ site	-20.4	9	3.3	1	1	1
Banwell Bone Cave	UK	Bison priscus	calcaneum	OxA-14136	59500	>	Banwell MAZ site	-20.3	10.8	3.2	1	1	1
Banwell Bone Cave	UK	Bison priscus	calcaneum	OxA-14138	53900	>	Banwell MAZ site	-20.7	10.6	3.1	1	1	1
Hunter's Lodge Inn Sink	UK	Bison priscus	scapula	OxA-13566	54800	>	Banwell MAZ site	-20.6	8.8	3.2	1	1	1
Goat's Hole (Paviland)	UK	Bison	not given	OxA-6932	32600	950	OIS3	-20.2	9.5	2.9	2	2	2
Kendrick's Cave	UK	Bovine	humerus	OxA-11726	12310	50	GI-1ed	-20	2.8	3.2	3	3	3
Goat's Hole (Paviland)	UK	Bison	not given	OxA-13435	30320	170	OIS3	-19.4	10.2	3.2	4	4	4
Goat's Hole (Paviland)	UK	Bison	not given	OxA-13418	31250	230	OIS3	-20.2	8.4	3.3	4	4	4
Goat's Hole (Paviland)	UK	Bison	not given	OxA-6924	31600	850	OIS3	-19.5	7.9	2.9	2	2	2
Goat's Hole (Paviland)	UK	Bos/Bison	not given	OxA-6926	26820	460	OIS3	-20.2	8.8	3	2	2	2
Goat's Hole (Paviland)	UK	Bos/Bison	not given	OxA-6925	29850	700	OIS3	-19.9	6.2	3	2	2	2
Foxhole Cave	UK	Bos/Bison	sacrum	OxA-25158	28310	290	OIS3	-22.1	3.5	3.2	5	5	5
Foxhole Cave	UK	Bos/Bison	scapula	OxA-25157	30750	390	OIS3	-19.5	5.5	3.2	5	5	5
Pin hole Cave	UK	Bovini	partial right tibia	OxA-11976	40720	390	OIS3	-20.4	2.5	3.3	1	1	1
Pin hole Cave	UK	Bovini	left radius/ulna	OxA-13591	48000	1000	OIS3	-19.8	6.6	3.1	1	1	1

Supplementary table 5 bibliography

1: Higham, T.G., Jacobi, R.M., Bronk Ramsey, C., 2006. AMS radiocarbon dating of ancient bone using ultrafiltration. Radiocarbon 48(2), 179–195.

2: Richards, M. P. 2000. Human and faunal stable isotope analyses from Goat's Hole and Foxhole caves, Gower. Pp. 71-75 in S. Aldhouse-Green (ed.), Paviland Cave and the "Red Lady": a definitive report. Western Academic and Specialist Press, Ltd.: Bristol.

3: Jacobi, R.M., and Higham, T.F.G., 2011. The British Earlier Upper Palaeolithic: Settlement and Chronology. AHOB. Developments in Quaternary Science: 14 ISSN 1571-0866

4: Jacobi, R.M. and Higham, T.F.G. 2008. The 'Red Lady' ages gracefully: new ultrafiltration AMS determinations from Paviland. Journal of Human Evolution, 55: 898-907.

5: Schulting, R.J., Fibiger, L., Macphail, R.I., McLaughlin, R., Murray, E.V., Price, C. and Walker, E.A. 2013. Mesolithic and Neolithic humans remains from Foxhole Cave (Gower, South Wales). Antiquaries Journal 93: 1-23.

